

**FY 2017 Annual Report and
4th Quarter Research Performance Progress Report**

Project Title: Pore Scale Control of Gas and Fluid Transport at Shale Matrix-Fracture Interfaces

Project Period: 10/01/16 – 09/30/18

Reporting Period: 7/1/17 – 9/30/17

Submission Date: 11/30/2017

Recipient: SLAC National Accelerator Laboratory

Recipient DUNS #: 00-921-4214

Address: 2575 Sand Hill Road, MS 69
Menlo Park, CA 94025

Website (if available) www-ssrl.slac.stanford.edu

Award Number: FWP 100211

Awarding Agency: NETL

Principal Investigator: Dr. John Bargar
Senior Staff Scientist
SLAC National Accelerator Laboratory
Phone: 650-926-4949
Email: bargar@slac.stanford.edu

Co-Principal Investigators: Dr. Gordon E. Brown, Jr.
Dr. Kate Maher
Dr. Anthony Kovchek
Dr. Mark Zoback

NETL Project Manager: David Cercone

TABLE OF CONTENTS

1.....	EXECUTIVE SUMMARY	3
2.....	GOALS AND OBJECTIVES	9
3.....	TECHNICAL HIGHLIGHTS	9
4.....	RESULTS AND DISCUSSION: TASK 2	10
5.....	RESULTS AND DISCUSSION: TASK 3&4a	18
6.....	RESULTS AND DISCUSSION: TASK 3&4b	24
7.....	REFERENCES	28
8.....	RISK ANALYSIS	29
9.....	MILESTONE STATUS	30
10.....	SCHEDULE STATUS	32
11.....	COST STATUS	34
12.....	COLLABORATIVE LEVERAGING	35
13	CONCLUSIONS	35
APPENDIX A	DELIVERABLES	36

1. EXECUTIVE SUMMARY

Hydraulic stimulation of unconventional reservoirs has transformed the U.S. energy economy and provided powerful technical capabilities to implement national energy policy, while reducing worldwide reliance on less environmentally friendly fossil fuels [1]. In spite of these achievements, unconventional production remains highly inefficient, with much of the resource remaining in place. This project is advancing microstructural-chemical knowledge regarding two important sources of inefficiency: (i) scale precipitation, which occludes fractures and matrix porosity, and (ii) the chemistry and microstructure of fracture-matrix interfaces, referred to here as *altered zones*, which act as gateways through which gas and oil must flow in order to be collected from the largely inaccessible reserve of hydrocarbons within shale matrix (*cf.* **Figure 1**). Our research is showing that the properties of the altered zone strongly influence chemical exchange between the shale matrix and fracture surfaces.

Fluids injected during unconventional stimulation react strongly with shale, dissolving and mechanically weakening fractures and proppant alike, driving scale precipitation, and initiating a cascade of organic-mediated and oxidation-reduction reactions. These reactions are of intense interest for their potential to reduce permeability and inhibit production. Importantly, they also offer a means to adaptively tailor geochemical reactions and matrix permeability in specific and desired fashions, to selectively arrest or accelerate scale precipitation, and to initiate and control chemical and physical processes that could be used to liberate more resource from the matrix. In order to prevent scale precipitation and improve control of fluid and gas flow, a commanding grasp of the geochemical factors that govern ‘keystone’ reactions such as barite and iron oxide precipitation and control of matrix access is critical.

The largely inaccessible interior of the shale matrix is a frontier research focus because it is the largest and mostly untapped reservoir for the hydrocarbon resources. For this reason, *even a small increase in fractional production from the matrix has the potential to deliver large absolute increases in production*. For example, increasing oil production from matrix by *ca* 5% would *double* production in an average well. The low permeability and diffusivity of the shale matrix is in many cases the most significant impediment to production. It is therefore paramount to understand chemical, microstructural, and permeability properties of the *altered zone* over time.

Knowledge gaps: Shale reservoirs are highly complex physically and chemically. As a community, we lack understanding of the fundamental geochemical and kinetic parameters that govern precipitation of ubiquitous scale phases such as barite in unconventional host rock during and following stimulation. We also lack basic physical-chemical numerical models to predict gas and fluid transport across the altered zone.

This project is conducting highly integrated reactive transport research across scales (from pores hundreds of nanometers in diameter to millimeter-dimension fractures) to address two crucial and interrelated reservoir performance needs that, if solved, have the potential to deliver major increases in efficiency:

- (i) Reducing scale precipitation through better understanding and control of fundamental geochemical and kinetic factors; and
- (ii) Improving microscale knowledge of the fracture-matrix interface required to develop chemical/physical manipulation approaches that can access resource in the matrix.

The objectives of this project: are to discover, quantify, and model fundamental geochemical controls over: (i) scale precipitation in fracture and matrix and; (ii) shale alteration induced by reaction with hydraulic fluids during stimulation. We are focusing our experimental effort at the scales (pores and microfractures) where mineral dissolution and precipitation occur and linking these microstructural-chemical changes to permeability. These goals have required us to address several significant research challenges, including (1) the development of approaches to image geochemical reactions occurring within shale matrix in three-dimensions over time, and at the sub-micron scale to deduce co-operative chemical effects between acid, organic compounds and metal and alkaline earth reactivity, and (2) the development of methods to measure matrix permeability (as opposed to fracture permeability) within altered zones of fluid-reacted shales. We are addressing these challenges by integrating a suite of high-resolution synchrotron- and laboratory-based x-ray tomographic and spectroscopic techniques, permeability measurements, geochemical experiments, and numerical reactive transport modeling.

The period under review comprises the initial year of a 2-year renewal project. During this period, we completed planning and literature review activities and initial scoping measurements and then initiated the full experimental program. At the present time, we are on-schedule and are already starting to write a manuscript to publish some of our new results on barite scale precipitation.

Scientific, technical, and personnel accomplishments during the performance period include:

- Publication of 3 manuscripts, with 3 additional manuscripts in preparation (Appendix A).
- Presentation of 10 research papers (1 invited) at national and international meetings, including: URTEC 2017, AIChE 2017, American Geochemical Union Fall Meeting 2016, and Goldschmidt 2017 (see Appendix A).
- Best Paper award for paper presented at the AIChE annual meeting, Oct 29- Nov 3, 2017, Session No. 644, Advances in Shale Characterization and Fluids Management
- Former postdoctoral researcher, Anna Harrison, hired as an assistant professor at Queen's University in Kingston, Ontario, Canada, with cross-appointments in the Departments of Geological Sciences and Geological Engineering and the School of Environmental Studies.
- Former postdoctoral researcher, Adam Jew, hired at SLAC as a research scientist.

Five key scientific discoveries have emerged from this work:

- 1) **pH is a master variable controlling the rate of barite scale precipitation, while commonly used chemical additives have unintended deleterious effects.** Barite scale precipitation is widespread in hydraulic fracturing systems and has the potential to significantly reduce the porosity/permeability of newly formed fractures, resulting in a significant negative impact on production. We have found that highly acidic conditions ($\text{pH} \leq 2$) completely halt barite precipitation, whereas at circum-neutral pH precipitation is fairly rapid. It is widely believed that barite scale precipitation can be controlled using additives to inhibit Ba^{2+} precipitation. However, we have found that organic additives used in unconventional shale reservoirs do not function as intended. Our work shows that the majority of additives do not slow barite scale precipitation, and in some cases they even increase barite scale precipitation rates. Thus far, no chemical additives investigated have

been able to completely halt barite precipitation. These findings emphasize the need to develop new approaches to control barite scale.

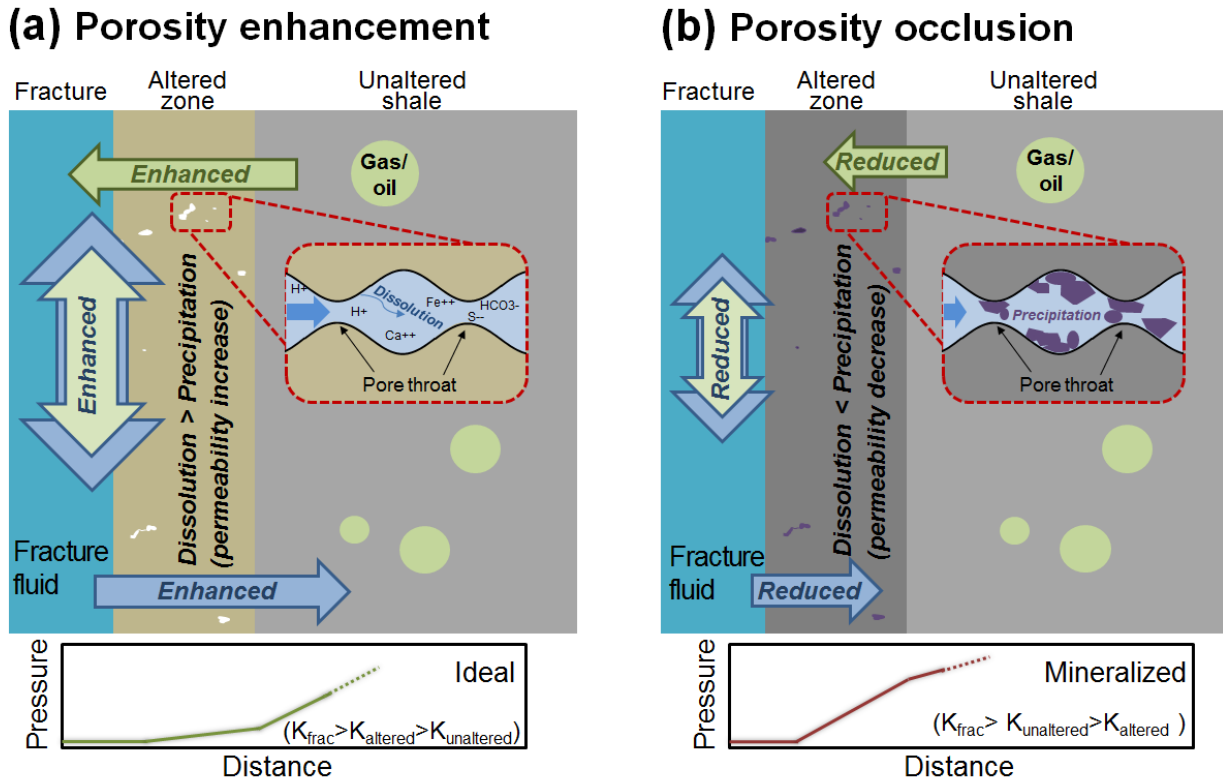


Figure 1: Conceptual model illustrating the altered zone at shale-fluid interfaces and the possible effects of dissolution and precipitation reactions on gas and water flow through the altered fracture surface. As seen in the left panel, when shales react with acidic solutions, increased porosity facilitates transport into the shale matrix, resulting in a concave up pressure gradient and enhanced recovery. Precipitation of secondary minerals in the altered zone (right panel) decreases permeability, leading to a concave down, and less ideal, pressure gradient.

- 2) **Drilling mud is a major source of Ba^{2+} in stimulated shale reservoirs, and this finding suggests that new scale control/drilling practices are needed.** One of the major findings of our work in the past year is that barite in the drilling mud (DM) is the most likely source of dissolved Ba^{2+} in fracture fluids. Barite is added to increase the overall density of the DM, which provides the critical safety function of preventing blow-outs during well development. Our studies show that barite in DM is unstable to acid and chemical attack from completion chemicals, causing Ba^{2+} to be released to solution. This new conclusion is of major practical significance to stimulation practices because it suggests that new chemical control strategies based on minimizing dissolution of barite in DM can be far more effective than current strategies that rely on inhibiting precipitation of already-dissolved Ba.

Schematic of Ba cycling in subsurface

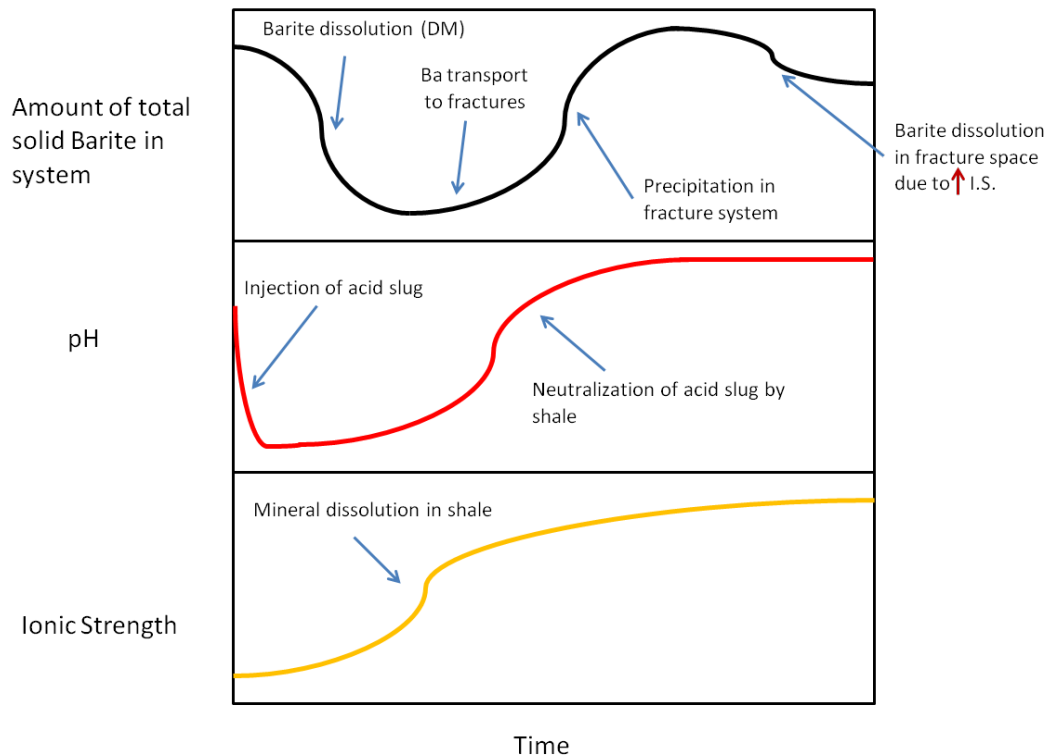


Figure 2: Schematic of Ba cycling in the subsurface based on barite precipitation reactions and Ba leaching experiments performed on drilling mud (DM). Amount of total solid barite in the system includes both the borehole with barite infused DM and the fractured shale/shale pores. The amount of Ra in solids mirrors the Barite curve in the upper panel.

- 3) **New conceptual model to predict and control barite precipitation in stimulated reservoirs.** Barium introduced to shale systems from barite-infused drilling mud will likely precipitate as fluid chemistry changes over time and is imbibed into the shale matrix. Another major set of conclusions from our work over the past year is that not only pH, but also ionic strength (I.S.), can strongly control barite precipitation kinetics. This finding leads to a new conceptual model for Ba^{2+} behavior during shale stimulation (**Figure 2**). In a hydraulic fracturing system an acid slug consisting of 15% hydrochloric acid is often injected prior to any other fracturing chemicals. This initial acid slug rapidly drops the pH of the system (**Figure 2**, middle panel) which subsequently is slowly neutralized by the dissolution of carbonate minerals (primarily calcite). The degree and rate of acid neutralization is dependent on the amount of carbonate in the host rock. As minerals in the rock dissolve (carbonates, pyrite, clays, etc.) during acid neutralization, the ionic strength of the solution will slowly increase (**Figure 2**, lower panel). These two key chemical parameters give rise to a complex Ba cycle (**Figure 2**, upper panel). As the acid slug interacts with the barite infused DM, a significant amount of Ba is released into solution (upwards of 25%) and forced into the newly formed fractures. As pH increases Ba will rapidly precipitate as barite on shale surfaces and in shale pores. Since acid neutralization increases faster than I.S., the I.S. inhibition effect will not occur unless very briny injection fluids are used. Once the barite

precipitates, a small fraction of the newly precipitated scale will be dissolved as I.S. rises to concentrations required for barite dissolution (**Figure 2**, upper and lower panels). Though some of the barite will dissolve (releasing trapped Ra), laboratory experiments and thermodynamic models predict < 10% of the precipitated Ba will be released back into solution. Because radium is incorporated into barite, the barium cycle also has important implications for radium concentrations in flow back water.

- 4) **The altered zone is much thicker than previously thought.** Due to the extremely low permeability of shale matrices, chemical reactions such as scale precipitation generally have been considered to be limited to fracture surfaces and fracture space. However, our whole-core experiments show that the alteration zone (**Figure 1**) can extend into the matrix by at least 0.5 cm within only 3 weeks. Moreover, the thickness of the altered zone and the extent of alteration varies as a function of the type chemical reactions occurring (*e.g.*, dissolution, scale precipitation, sulfide oxidation), the mineralogical composition of the shale, and the shale-fluid interfacial microstructures. The upper bound of 0.5 cm for the thickness of the altered zone observed in these measurements was limited by the 1 cm diameter of the cores used in the experiment. In the real systems, the altered zone thickness is likely to be even greater. This finding suggests that alteration of porosity/permeability occurs in a much larger zone in shale formations than we previously expected and that it is technically feasible to access matrix space for enhanced production.
- 5) **Chemical alteration is controlled by microcracks and presence of surface scale coatings.** Our whole-core experiments show that chemical alteration in the fluid-matrix interface, which is directly related to porosity/permeability alteration, depends heavily on the presence of micro cracks and surface scale coatings. We observed that shale cores containing microfractures exhibited deep alteration. On the other hand, the presence of thin (< 50 μm) layers of barite scale on the shale surface significantly reduced development of the alteration zone due to dramatically diminished diffusion across the shale-fluid interface. These processes provide 'control points' where process optimization can reduce formation damage and simultaneously show that altered zone transport properties can in principal be controlled through chemical manipulation.

Impact and future directions. We have made significant strides in understanding chemical reaction networks occurring in stimulated shale reservoirs, and of critical chemical parameters (shale mineralogy and fluid chemistry) that govern these reactions. Our findings emphasize the need to develop new stimulation practices that control scale and thus enhance resource extraction.

The prominent role played by pH in controlling scale precipitation (both precipitation rates and behavior, *i.e.* crystal size and type) indicates that different shale formations, which have different pH buffering capacities, are a major factor to be taken into consideration when designing enhanced stimulation procedures. Beyond differences in rock pH buffering capacities, there are significant variations in "average" fracture fluid formulations used in different shale plays. It is crucial to understand how shale samples from various shale plays respond to their respective fracture fluid formulations.

Our research thus far has produced important knowledge about fracture fluid-shale interactions, but has focused on specific fracture fluid formulations and shale compositions encountered in the Marcellus region. There is thus a need to extended this successful approach to

investigate fluid-shale reactions in important producing shale reservoirs such as Bakken and Wolfcamp, but also developing plays such as Mancos and Shublik, HRZ (High Radiation Zone, Alaska), taking into account their respective fracture fluid compositions. Representative fracture fluid formulations containing the most common (> 80% of wells criterion) and reactive additives within the region can be created from data available at FracFocus. Such studies would make it possible to identify important fundamental issues related to scale formation, opening the door to optimized fracture fluid chemistry and drilling practices that would improve short- and long-term production. We envision submitting a renewal proposal that would include research to address this important need, using and evolving the methodology that we have developed (laboratory-, synchrotron, X-ray and electron microscopy-based techniques to identify porosity and permeability changes). Other strategic research needs that can be addressed in a renewal activity will be discussed with NETL management.

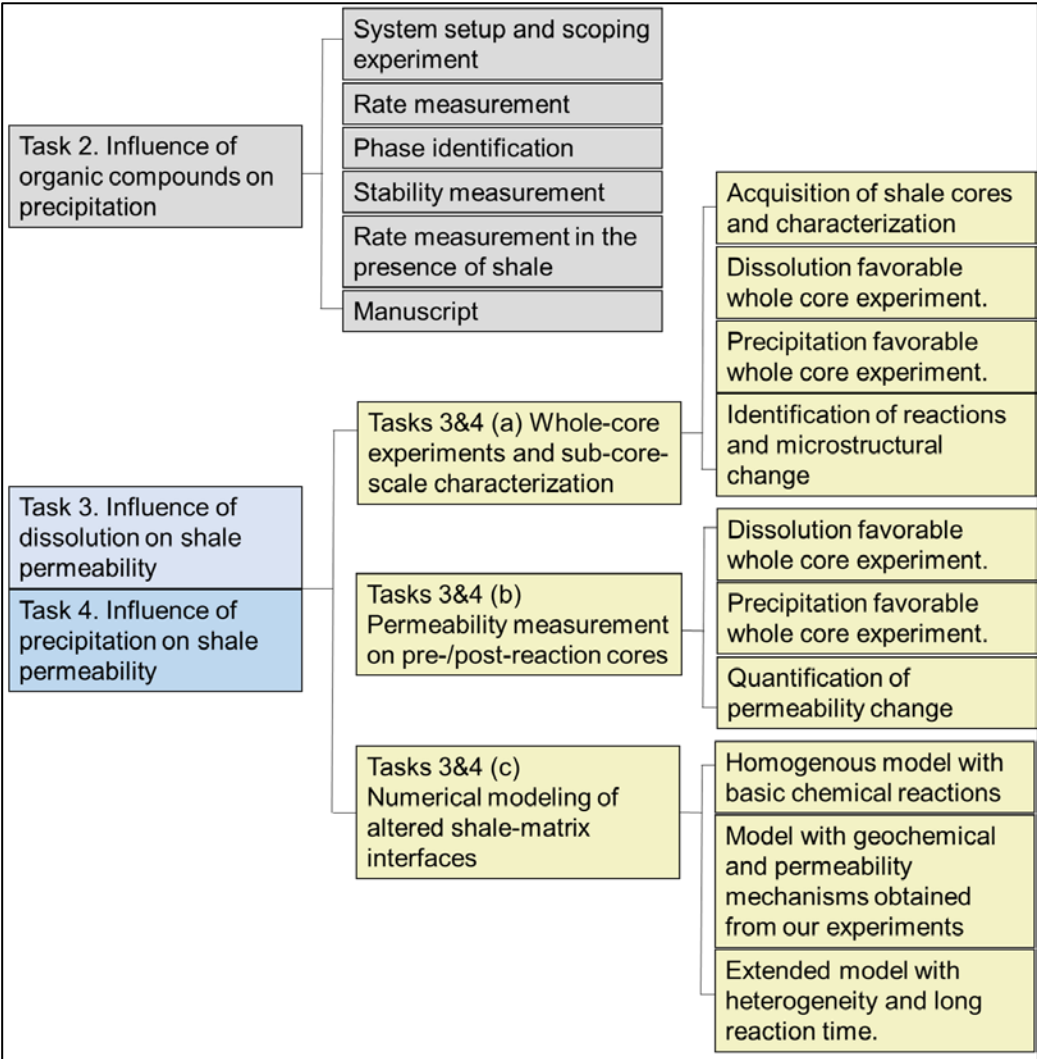


Figure 3. Structure of this report and the relation to PMP tasks. Task 1 (not illustrated) is the program management activity.

2. GOALS AND OBJECTIVES

The overarching goal of this project is to discover new fundamental knowledge about: (i) geochemical and kinetic controls over secondary mineral precipitation; and (ii) fluid-induced chemical/microstructural alterations to shale interfaces and their impacts on permeability and gas/fluid transport. We are accomplishing these goals through a suite of activities that integrate synchrotron-based imaging and CT methods, electron microscopy, permeability measurements, and geochemical and reactive transport modeling. This approach provides the capability to associate pore- and fracture-scale geochemical processes to resultant changes in transport properties.

Task 1 encompasses project management activities. The three scientific tasks defined in our project management plan are (**Figure 3**): **Task 2**: Characterizing the influence of dissolved organic compounds, pH, and ionic strength on barite scale precipitation. In contrast, **Tasks 3 and 4** are focused on characterizing and modeling the chemical/microstructural alteration of shale-fracture interfaces and the impact of this alteration on gas transport. **Task 3** is nominally oriented toward porosity generation within the altered layer ('dissolution favorable' conditions, Figure 3), whereas **Task 4** is focused on secondary mineral precipitation within the altered layer ('precipitation favorable' conditions). These two chemical processes are interrelated (dissolution leads to precipitation), and the work flows for subtasks 3 and 4 are similar. Consequently, Task 3 and 4 efforts have been merged and are reported in section 3 (this section) as "**Task 3&4**". The merged work flow for **Task 3&4** self-organizes into 3 primary activities: (a) Chemical reactions and sub-core-scale geochemical characterization; (b) permeability measurement, which requires whole-core characterization using core-flood approaches; and (c) numerical modeling of altered shale-matrix interfaces. Results for each are presented separately later in this section. Effort for **Task 3&4** in Year 1 has focused on activities (a) and (b), whereas numerical modeling will be a more significant focus in Year 2.

3. TECHNICAL HIGHLIGHTS

Task-by-task highlights of accomplishments in FY 2017:

Task 1

1. The project management plan was developed, submitted, and approved.
2. Teleconference and in-person meetings with research scientists at NETL.

Task 2

3. Ba precipitates have been analyzed using x-ray diffraction (XRD) to determine the phase of Ba precipitated in organics reactors.
4. Ba precipitate particle size was determined using dynamic light scattering (DLS).
5. Leaching experiments of Barite crystals and Ba-enriched drilling muds from the MSEEL site in the presence of various pHs, I.S.s, and organics was completed.

6. Barite precipitation experiments under various solution chemistry conditions (pH, ionic strength, organics) were completed.
7. Identification of the most important chemical parameters for barite precipitation were identified.
8. Kinetic rates for barite precipitation were calculated and compared to literature values.

Tasks 3 & 4 (a) Fundamental precipitation and dissolution reactions controlling porosity

9. Scoping experiments were conducted to choose experimental conditions and to develop characterization methods using lab and synchrotron techniques.
10. Whole core experiments were conducted with New York Marcellus, Pennsylvania Marcellus, and Eagle Ford.
11. XRD data were collected for pre- and post-reaction cores to compare the bulk mineralogy alteration.
12. Micro CT data were collected and processed for pre- and post-reaction cores using Zeiss Xradia 520 Versa X-ray CT with voxel size of 5 μm .
13. Synchrotron x-ray fluorescent (XRF) Fe and S maps and spectra were collected from shale samples in Quarters 1-3.
14. Small angle x-ray scattering data were collected at SSRL Beamline 1-5.
15. Synchrotron x-ray μ -XRF Fe maps and spectra were collected from SSRL beamline 2-3 in July for pre- and post- reaction shale core cross-sections in Quarter 4.
16. Synchrotron x-ray μ -XRF Fe and S data from cross-sections of the pre- and post-reaction cores were analyzed.
17. Duplicate experiments were conducted in September, and samples are pending characterization.

Tasks 3 & 4 (b) Measuring permeability alteration

18. Test and develop methodology for Permeability of unreacted Marcellus and Eagle Ford cores were measured.

Details of task progress:

Task 2: Effects of dissolved organic matter on the precipitation and stability of secondary mineral phases

Barite (BaSO_4) scale precipitation is a prime concern in nearly all hydraulic fracturing systems, both in shale bodies and in piping, because of its ubiquitous presence and low solubility, tends to be over-saturated. Barite is added to drilling muds (DM) at high concentrations (> 10 g/kg) in order to increase the density of the muds and aid in the drilling process [2-4]. Even though some operators attempt to remove as much of the drilling mud as possible, significant

amounts of DM is imbedded in the rock during the drilling process remain. This leftover DM can then react with the initial hydrochloric acid slug (~15%) injected down bore hole to clean up perforations in the bore casing and to help clean out the drilling mud. In comparison to the drilling mud, barium concentrations native to the shale host rock are lower, typically ≤ 1 g/kg in the solid [5]. The high volume/pressure of the injection fluid and the low pH (\sim pH 0), result in a high probability of dissolving and mobilizing Ba from the DM and forcing it into the newly formed fractures as well as the shale matrix itself. This introduction of significant quantities of Ba^{2+} and SO_4^{2-} , including that which is leached from the shale itself, will lead to scale production, clogging of newly developed secondary porosity, and overall attenuation of permeability.

As shown in our recent paper in *Energy and Fuels* [6], soluble organic compounds in hydraulic fracturing fluids can strongly accelerate the formation and mineralogy of Fe(III)-bearing scale. We posit that natural organics will similarly modify the formation of barite scale. Moreover, significant quantities of various organics such ethylene glycol are injected into the subsurface to prevent scale precipitation. Due to the large number of possible interactions, it is likely that these compounds can modify the rate and extent of scale precipitation.

The scope of this task includes investigating the effects of various classes of added and natural organics found in hydraulic fracturing systems, including fracture fluid additives (biocides, breakers, crosslinkers, friction reducers, scale inhibitor, Fe-control, corrosion inhibitor, and gellants), as well as those present in shale (both formation and produced waters). As experimental work has progressed, we have observed that ionic strength (I.S.) and pH are particularly important parameters because they can vary strongly during hydraulic stimulation. **However, no previous experiments have directly measured barite solubility under fracture-relevant conditions.** Subsequently, experiments detailing the importance of ionic strength have been carried out to determine its impact on barite precipitation at various times during the hydraulic fracturing process. The highest ionic strength we used is set at ~ 2.6 M NaCl (~ 90 g/L TDS), which is consistent with measured Na concentrations in produced waters [7-8]. Additionally, significant work has been accomplished to determine the source of Ba in these systems in hopes of finding a solution that will reduce the amount of Ba introduced into the subsurface. This portion of the experimental space also includes determining which chemical parameters that are most important for Ba release from the host shale, drilling mud, and pure barite crystals (experimental control).

Major questions being addressed by this task are, how do variations in pH, ionic strength, dissolved organic compounds, and mineral surface area impact Ba release into hydraulic fracturing systems and subsequent barite scale precipitation?

Review of progress in quarters 1-3: Barium Precipitation

Effect of pH. Of all the chemical parameters tested, pH had the greatest impact on Ba precipitation (**Figure 4**). At pH 2 and lower no Ba precipitation was detected. As pH increased, Ba precipitation rates increased, until pH 5 was reached. Surprisingly, once solution pH reached 5, there was no difference in precipitation rates up to pH = 7 (**Figure 4**). The calculated rate constants for the various pH reactors at 80°C were 1-1.5 orders of magnitude faster than literature values [9-13] calculated at 25°C . In general, chemical reactions double in rate with every 10°C increase in temperature, which would result in a increase in reaction rates of 1-1.5 orders of magnitude.

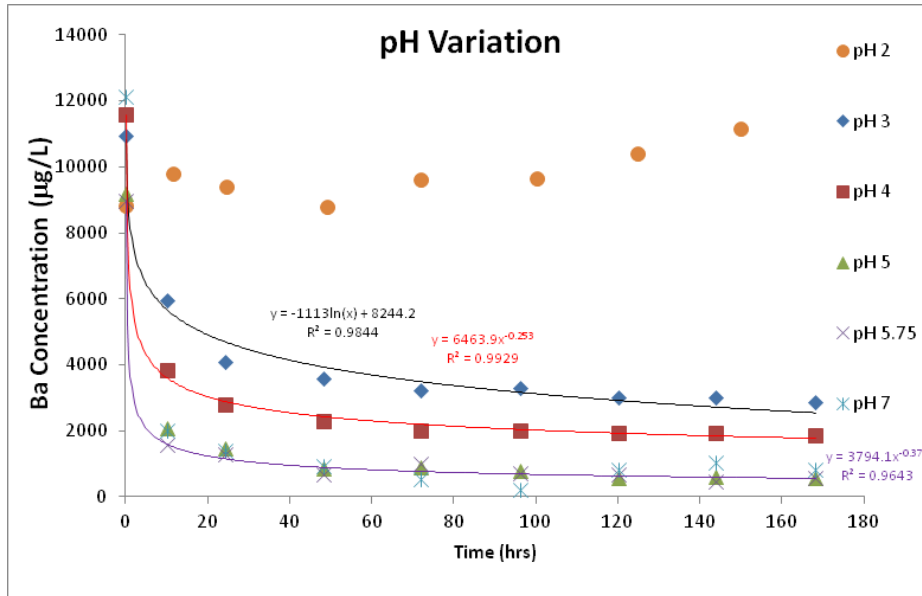


Figure 4: Barium precipitation with varying initial pH conditions. Ionic Strength with corresponding saturation indices (in brackets) for the various pH reactors: 0.596 mM [S.I. = 1.235] (pH 7), 0.597 mM [S.I. = 1.235] (pH 6), 0.6 mM [S.I. = 1.233] (pH 5), 0.64 mM [S.I. = 1.212] (pH 4), 1.07 mM [S.I. = 1.042] (pH 3), and 5.96 mM [S.I. = 0.345] (pH 2).

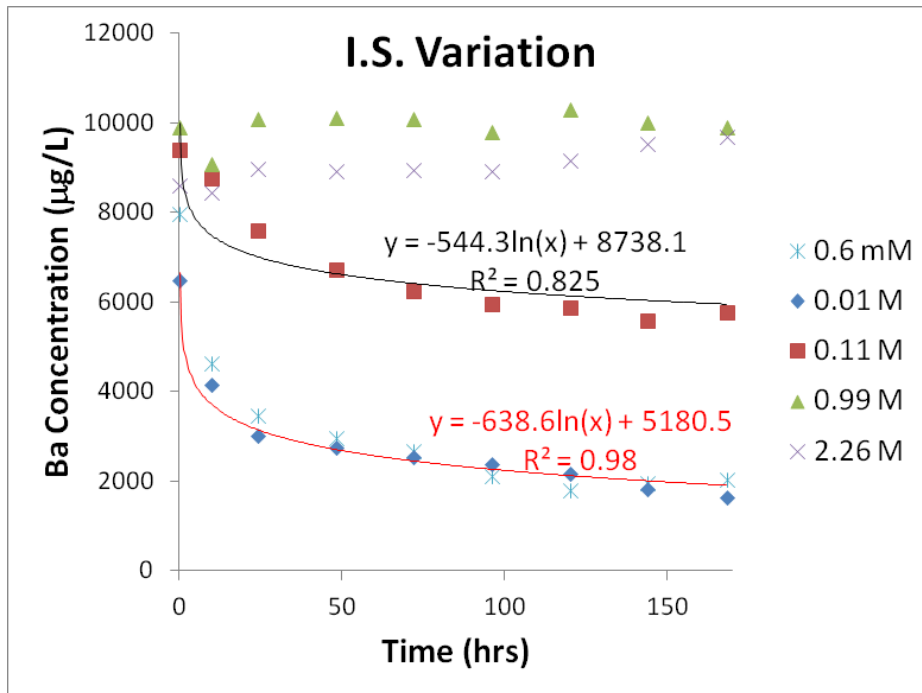


Figure 5: Barium precipitation with various ionic strengths. Initial Ba concentration for reactors was 10000 ppb. Error for measurements is < 8%.

The experimental solubility results for various pH's at 80°C are inconsistent with thermodynamic modeling, where model results indicate that there should be differences in precipitation trends for pH's 5, 6, and 7. Numerous experimental runs using identical conditions show a high reproducibility of these experiments, suggesting that the values in the thermodynamic database for Ba complexation and precipitation are incorrect for these systems.

Effect of ionic strength. When ionic strength was varied using NaCl, differences in precipitation trends were observed at the upper range of salt conditions, *i.e.*, between 0.01 and 0.99 M (**Figure 5**). However, at low I.S., < 0.01M, the precipitation rates were identical (**Figure 5**). These results do not conform with thermodynamic calculations which indicate that there should be a difference in the amount of Ba precipitated as barite between 0.6 mM (where 69% of the total Ba²⁺ should precipitate) and 0.01 M (where 65% of the total Ba²⁺ should precipitate). As I.S. approached concentrations similar to produced waters, *i.e.*, > 1M, no Ba precipitation was detected in the reactors (**Figure 5**). This complete inhibition of barite precipitation does not agree with thermodynamic modeling where steady state Ba concentrations should drop from 8500 ppb to ~6000 ppb. This observation indicates that high I.S. kinetically inhibits the nucleation of barite crystals from a homogenous solution, *i.e.*, in the absence of shale mineral surfaces (**Figure 5**). The conclusion that I.S. kinetically inhibits nucleation is consistent with the DLS measurements described above.

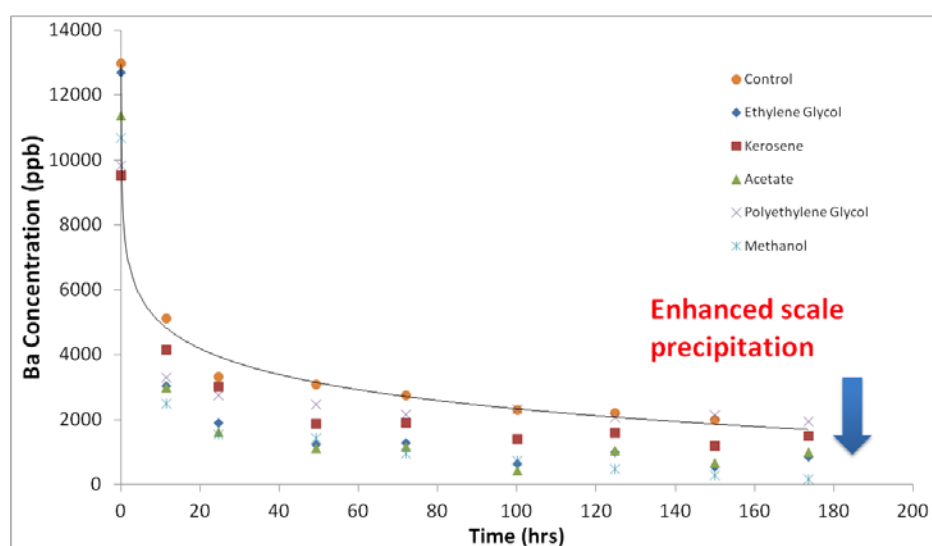


Figure 6: Ba precipitation reactor results for select organics showing enhanced scale precipitation.

Effect of organics at pH 7. Organics added to the barite precipitation experiments had an unexpected effect. Since specific organics such as ethylene glycol are added to control barite scale, the assumption is that these chemicals would completely, or at least retard, barite precipitation. In systems with simple organics (**Figure 6**), all organics added either had no impact on precipitation rates compared to the control experiment or increased reaction rates. What is very surprising is that the ethylene glycol that is added specifically to inhibit scale production actually enhanced scale production. In extreme cases, ammonium persulfate (breaker) and 2-ethyl-1-hexanol (corrosion inhibitor), Ba precipitation is rapid with full

precipitation occurring within a 24 hour period (data not shown). This is not overly surprising since ammonium persulfate decomposes releasing significant quantities of SO_4^{2-} resulting in supersaturation with regards to barite.

When organics with a higher chelating potential, citrate and guar gum, are used in Ba precipitation reactions the rate of precipitation was retarded (**Figure 7**). The striking thing with the experiments using organics is that in every situation barite precipitation was never completely halted. These results are even more concerning when compared to a real world system since these idealized experiments have a significantly lower saturation index compared to the real world systems where Ba in produced waters are 10-100x that which were used in this work.

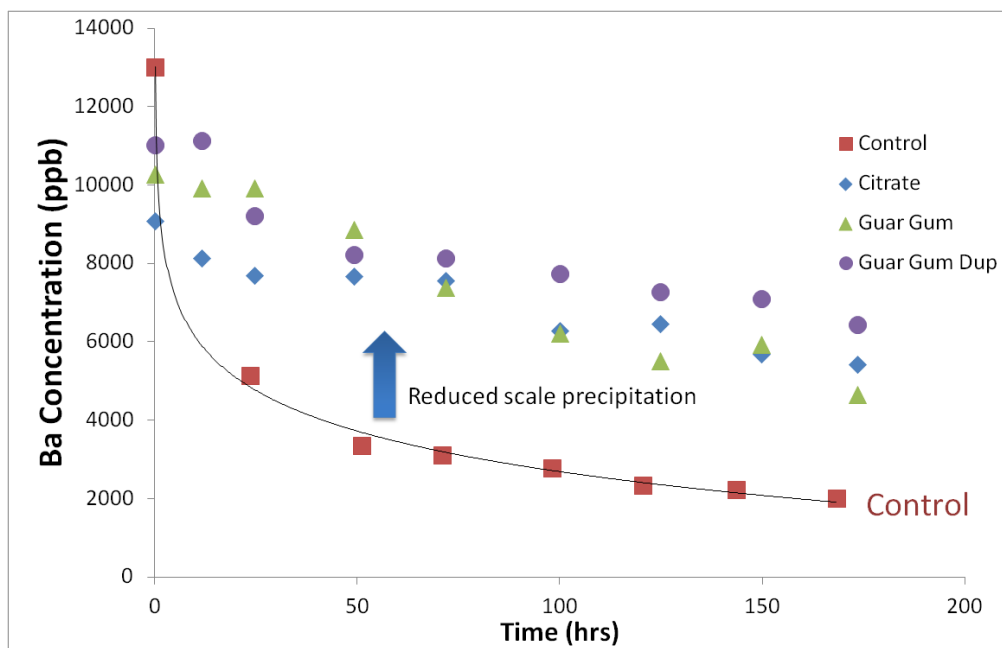


Figure 7: Barium precipitation experiments using strongly chelating organics.

Progress in quarter 4

Barium precipitation experiments were upscaled in order to increase the quantity of Ba precipitates created in order to determine the type of Ba-phase created and average particle size. Reactors containing pure barite were reacted with varying pH, I.S., and organic conditions to determine the amount of Ba that could potentially be released into solution. Additionally, because drilling muds from the MSEEL site, contain 20-30 wt.% barite, the DM was used in similar leaching experiments to determine whether leftover drilling mud in the borehole could be a potential Ba source to the system. These leaching experiments will help determine if the major source of Ba in these systems is from the leftover drilling mud rather than the shale itself.

Results: Barium precipitate mineralogy and particle size. Thermodynamic modeling of the various Ba precipitation experiments indicate that in all systems in which Ba will precipitate, barite will be the most stable phase. Due to the low yield of solids from the 40 mL reactors, the experiments were upscaled using 240 mL bottles. The precipitates were collected via

centrifugation, pouring off the supernatant, and then drying in a desiccator under vacuum. The solid material was analyzed using both XRD (mineral phase) and DLS (particle size). The XRD pattern from the control experiment matched that of the barite control sample (**Figure 8**). Diffractograms for all of the other Ba precipitation reactions also showed precipitation of barite (Glutaraldehyde used as an example, **Figure 8**) indicating that in all the reactors in which Ba precipitated, only barite precipitated. Dynamic light scattering measurements of the crystalline material was completed in order to determine average crystal sizes. The samples were sonicated for 30 minutes to break up mineral aggregates. Because barite has a density, 4.5 times that of water, only 5 scans (rather than the normal 25) were able to be collected before the majority of the barite crystals moved out of the laser path and settled on the bottom of the sample cuvette. Surprisingly, in all cases the average barite crystal size was $1.7 \pm 0.2 \mu\text{m}$. This indicates that variations in Ba precipitation in the presence of different organics *is due primarily to inhibition of barite nucleation and not surface poisoning*. If surface poisoning were the main reason for differences in the Ba precipitation then a much larger distribution of particle sizes would be expected. The XRD results conform to thermodynamic modeling while the DLS measurements show that the type of organics in the systems have no effect on particle size. These results suggest that to control barite precipitation in these systems, control strategies need to focus on inhibiting barite nucleation rather than poisoning the surfaces of the barite crystals.

Table 1: Task 2 objectives for quarter 4

Goal	Status
Crystal phase of Ba precipitates determined using XRD	Complete
Average crystal size of Ba precipitates determined using DLS	Complete
Leaching experiments of Barite using various pH, I.S., and organics	Complete
Leaching experiments of Ba-enriched drilling muds using various pH, I.S., and organics	Complete
Initial draft of manuscript	In progress

Barite/Drilling Mud Leach Experiments. Pure ground barite and barite-infused drilling mud from the MSEEL research site were reacted with solutions of various pH, I.S., and organic formulations at 80°C for 72 hrs. For the leaching of pure barite, 0.1 g of ground barite (~1 μm in diameter) was reacted in 40 mL of solution. The MSEEL drilling mud (DM) contained 20-30 wt.% barite (information from the MSDS) and reactors contained 0.2 g of the wet mud (samples were identical to those used in drilling operations) in 40 mL of solution resulting in 0.04-0.06 g of barite used per reactor. As seen with the barite precipitation experiments, pH is the master variable for barite stability (**Table 2**). The 15% HCl extraction mimics the initial acid slug in hydraulic fracturing operations and was responsible for liberating 6% of the total Ba from pure barite and 15.6 - 23.0% of the total Ba from the drilling mud. When the amount of barite in the DM reactors is normalized to the pure barite reactors it is seen that the barite in the drilling mud is more susceptible to dissolution than its pure barite counterpart. Circum-neutral pH had very little impact on Ba released into solution for both barite and DM. Ionic strength did have a strong impact on barite dissolution, but to a lesser degree than pH. Though I.S. is low when

freshwater is used in completions, as I.S. increases throughout the production process, a portion of the precipitated barite will dissolve re-opening a portion of the pores and surfaces clogged by barite scale, but also potentially releasing Ra captured during the precipitation process (**Figure 1**, upper panel). Organics had very little impact on barite dissolution. The only organic tested that dissolved more of the pure barite compared to the other organics was glutaraldehyde (a common biocide) which has been previously shown to slow barite precipitation. Conversely, ammonium persulfate released the least amount of Ba into solution due to the increased concentration of SO_4^{2-} in solution, which reduces the solubility product (thermodynamic inhibition). This result is consistent with the precipitation reactions discussed in the 3rd quarter report in which 2/3 of the Ba precipitated within the first 6 minutes of the experiments. Of particular interest is the fact that the pH 2 fracture fluid was able to solubilize more of the barite in both the pure barite and DM systems than just pH 2 solution (**Table 2**). This suggests that organics, most likely the guar gum, in the fracture fluid is chelating Ba released into solution which would allow more barite to dissolve in order to reach equilibrium. The total amount of Ba released from the DM with full fracture fluid far exceeds that of the shale itself where at 3 weeks the maximum Ba

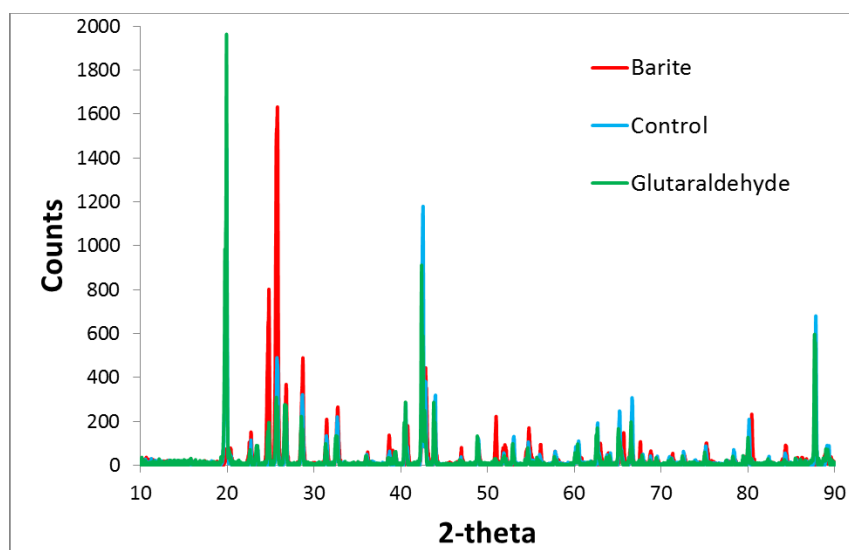


Figure 8: XRD diffractograms of Barite, Control reactor, and reactor containing Glutaraldehyde. Differences in peak intensity is due to preferential layering of the ground samples on the sample slide.

concentrations in solution for the sand sized shales were 148.9 ppb (Barnett), 302.5 ppb (Eagle Ford), and 273.3 ppb (Marcellus). These results show that the drilling mud is the most likely source of Ba in these systems and the barite contained in the DM is more prone to dissolution than pure ground barite. These results indicate that a change in drilling process is needed. Since we have shown that all organic additives added to fracture fluids do not inhibit barite precipitation, the focus for controlling Ba in these systems is to keep Ba in the DM from being released during the completion. There are several options that can be suggested for addressing issues with Ba leaching: (1) replace barite with another weighing agent, (2) remove acid from the completion chemical recipe, (3) change the type or concentration of the acid injected, or (4) add a chemical to the completion to either stabilize the barite or chelate released Ba. This point will be addressed during our project renewal period.

	Barite (mg/L Ba)	Drilling Mud (mg/L Ba)
A. Organic and inorganic additives:		
Citrate	1.5	
Guar Gum	1.6	
Ethylene Glycol	1.3	2.4
Polyethylene Glycol	1.8	1.1
Marcellus Bitumen	1.8	
Acetate	2.3	1.3
Benzene	2.3	
Kerosene	1.8	
Methanol	2.1	1.2
Glutaraldehyde	3.4	1.5

Ammonium persulfate	0.18	0.2
B. Fracture fluid	9.4	4.0
C. Ionic strength/pH		
I.S. 0.01	2.8	1.2
I.S. 0.1	5.1	2.2
I.S. 1	13.9	6.7
I.S. 2.3	22.2	11.4
pH 7	2.0	1.4
pH 5	2.0	
pH 4	2.2	1.5
pH 2	6.4	2.9
15% HCl	88.8	136

Table 2: Barium leach experiments on ground pure barite and MSEEL drilling mud. Concentrations of dissolved Ba are given in units of mg Ba per L solution. A. Impact of isolated organic additives in water, B. Impact of ionic strength, and C, pure water with added HCl.

Planned Experiments. At this time only one more set of experiments is required for the manuscript. These experiments will consist of measuring the sorption rate of Ba²⁺ to shale surfaces to compare with barite precipitation rates in the presence of shale. If the Ba uptake rates in both experiments are similar, then that would indicate that sorption is occurring faster than precipitation and that precipitation on and in the shale is occurring following sorption of Ba.

Manuscript plans. A manuscript detailing the effect of various organics on the precipitation of barite at various ionic strengths is planned. The manuscript will also include variations, if there are any, to the speciation and crystallinity of Ba-bearing precipitates. A tentative title for this manuscript is: Organic and ionic strength controls on barite precipitation in hydraulic fracturing systems. Additionally, an abstract has been submitted to URTeC that will be later be expanded into an extended abstract for publication entitled: Barium Sources in Hydraulic Fracturing Systems and Chemical Controls on its Release into Solution.

5. Task 3&4 (a): Fundamental precipitation and dissolution reactions controlling porosity

Upon exposure to acidic fracture fluid, shale matrices can experience mineral dissolution, which leads to build-up of dissolved mineral-forming solutes in solution, accompanied by a slow rise in pH. These changes create the conditions favorable for precipitation of secondary minerals to occur. Both sets of processes (dissolution and subsequent mineral precipitation) can profoundly alter porosity, diffusivity, and permeability of the matrices, which may either enhance or reduce gas/oil production. At the present time, we can't predict which results will occur because we don't know the critical properties of the shale-fluid interface (such as thickness, porosity, and chemical and physical microstructure) and how the processes are distributed across it. A major consequence of this lack of knowledge is that we cannot design chemical processes to engineer and improve extraction of hydrocarbons from matrix. This discussion highlights the need to elucidate the impacts of geochemical reactions in shale on their porosity and permeability.

In this section we conducted whole core reactions and characterized them with μ -X-ray CT and synchrotron μ -XRF chemical imaging to characterize porosity changes, the thickness of the altered zone, the specific dissolving phases (e.g., carbonate and pyrite) and precipitating phases (e.g., Fe/Al oxides and Ca/Ba sulfate), as well as the spatial distribution of these reactions within pore structure. **Table 3** lists the experimental conditions employed in this task. In the 'sister' task (Task 3&4 (b)), reaction-induced permeability alteration of the shale matrix will be quantified with laboratory-based porosity and permeability measurements and connected back to this task to relate microstructural changes to permeability. This activity also strongly links to the results of Task 2, which are required to interpret and explain the whole-core results. In aggregate, this project will provide insights required to improve chemical manipulation of shale interfaces and to improve hydrocarbon extraction from matrix.

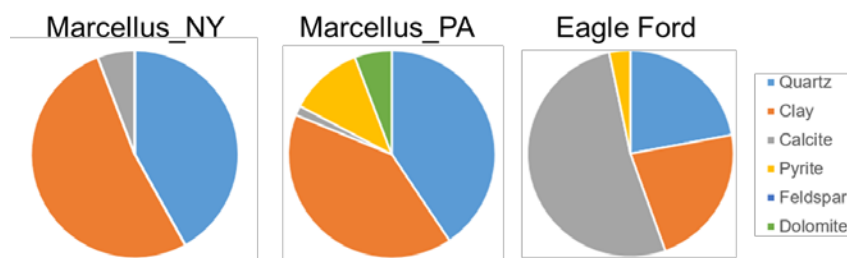


Figure 9. Mineralogy composition analyzed using XRD

Review of progress in quarters 1-3

Initial scoping experiments and sample characterization were performed in Q1 and Q2. Based on scoping experimental results, we finalized the conditions for dissolution and precipitation experiments, which are shown in **Table 3**. New experiments were conducted in Q3. Three types of shale were reacted, including Marcellus from New York and Pennsylvania, and Eagle Ford. After three weeks of reaction at 80 °C and 77 bars, the post-reaction micro-CT images (Zeiss Xradia 520 Versa X-ray CT) were compared with pre-reaction images. After CT scans, post-reaction cores were cross sectioned for synchrotron x-ray bulk spectroscopy and microprobe mapping. Bulk mineralogy analyses before and after reactions were conducted using x-ray diffraction.

Mineralogical composition. The New York Marcellus shale has high clay content, and very low carbonate content (*i.e.*, carbonate was not detected in XRD analyses). Pennsylvania Marcellus also has clay content and low carbonate content. Eagle Ford had high content of carbonate in the form of calcite. The XRD results are shown in **Figure 9**.

Reactivity of shale, effects of carbonate content, and secondary precipitation. The comparison of pre- and post-reaction cores is shown in the CT cross section images in **Figure 10**. The dissolution-favorable condition uses pH 2 fracture fluid as the reaction solution, whereas the precipitation condition uses pH 2 fracture fluid with additional 2 mM BaCl₂ and 0.06 mM Na₂SO₄ ($SI_{\text{barite}} = 1.3$) to more closely represent produced water compositions, which promote barite scale formation.

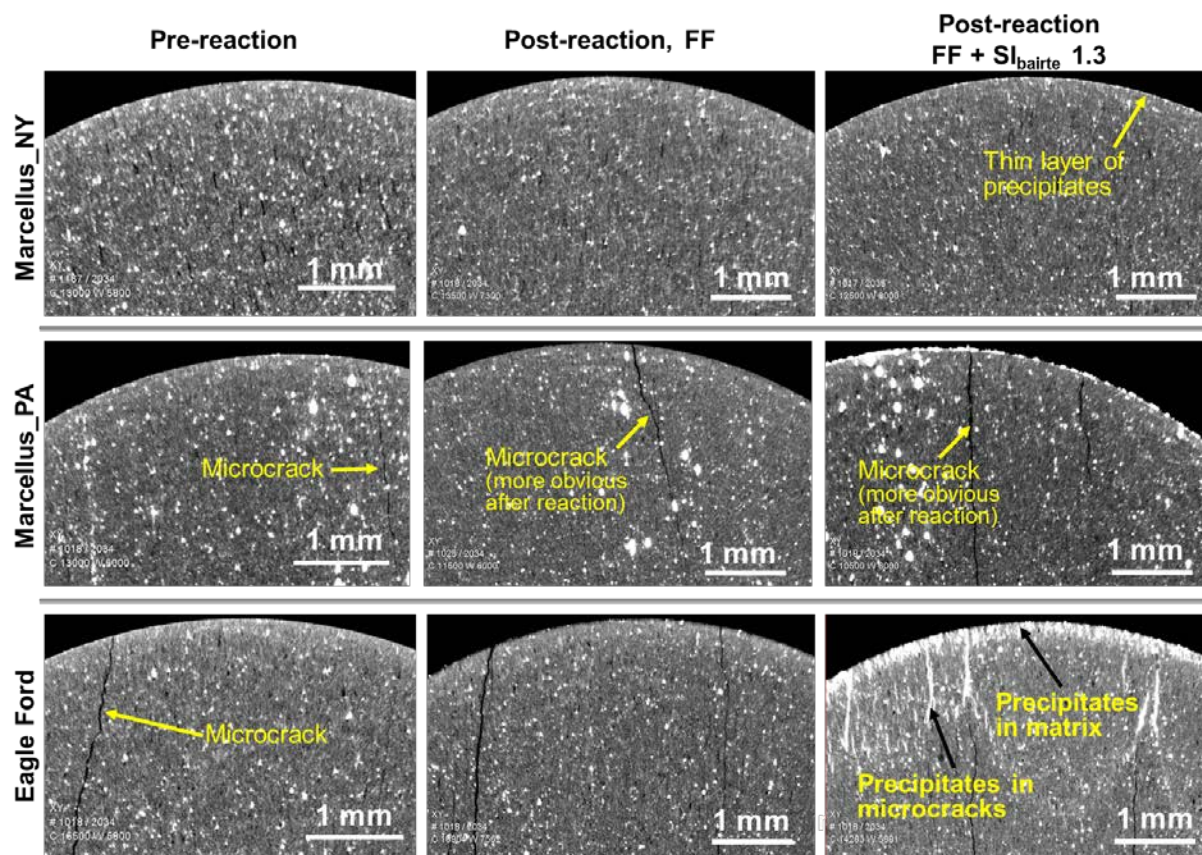


Figure 10. Comparison of pre- and post-reaction cores from micro-CT cross section images. Pixel sizes are 5 μm . The grey scale were adjusted for each image for the best image quality. The reaction conditions can be found in **Table 3**, and the mineralogic information can be found in **Figure 9**.

The New York Marcellus cores did not have any microcracks. A thin layer of barite precipitation was present on the core surface for the precipitation-favorable condition. Otherwise, the post-reaction cores did not show obvious differences from the pre-reaction cores, indicating that hardly any reaction took place in the shale matrix. The low reactivity is also evidenced by the pH alteration in the fracture fluid. After reaction, the pH of the fracture fluid remained at ~ 2 .

Table 3. Reaction conditions for whole-core experiments

Composition	Shale Type	Explanation
Dissolution-Favorable Experiments (Task 3)		
FF, No additional NaCl SI(barite)= 0.0	Marcellus (NY) Marcellus (PA) Eagle Ford	Expect that porosity alteration is controlled by calcite and pyrite dissolution
Precipitation-Favorable Experiments (Task 4)		
FF, No additional NaCl + 2 mM BaCl ₂ + 0.06 mM Na ₂ SO ₄ SI(barite)=1.3	Marcellus (NY) Marcellus (PA) Eagle Ford	Expect that porosity alteration is controlled by barite precipitation

* Fracture fluid (or FF) has a pH of 2 and contains chemicals listed in Table 5 in Quarter 1 Report. The composition is based on NETL's Greene County, PA Marcellus Well E.

The Pennsylvania Marcellus cores had microcracks, and these microcracks were more obvious after reaction for both the dissolution- and precipitation conditions. The post-reaction fracture fluid had pH ~ 3 compared to pH ~ 2 before reaction, indicating that dissolution had consumed acid. Similar to New York Marcellus, a thin layer of barite precipitates was observed on the external core surface in the precipitation-favorable case. From the synchrotron μ -XRF S map shown in **Figure 10**, it is obvious that the barite precipitates formed about 40 μ m deep from the core surface into the matrix, which is not resolved in **Figure 13**. No secondary precipitates were observed in microcracks. Comparing Marcellus cores from New York and Pennsylvania, we conclude that the reactivity of the shale heavily depends on the abundance of microcracks.

Eagle Ford had high contents of calcite, which is highly soluble under the acidic conditions commonly induced in stimulated formations. The post reaction fracture fluids in both reaction conditions had neutral pH's around 6. As evidenced in the barite precipitation experiments in **Task 2**, high pH promotes barite precipitation. As a result, a significant amount of barite precipitated in the precipitation-favorable conditions. Surprisingly, these secondary precipitates extended from the core surface into the matrix for ~ 400 μ m when there were no microcracks, and for 1 – 2 mm when there were microcracks. We expect that these pore-clogging secondary precipitates reduce core permeability significantly, and we will test this hypotheses in **Task 3&4 (b)**. These findings are consistent with our findings in Task 2, which showed that barite precipitation is fastest at near-neutral pH values, which are expected to occur in carbonate-rich systems such as Eagle Ford.

Progress in quarter 4

Six whole cores (1 cm in diameter, 2 cm long) drilled from Marcellus or Eagle Ford shale were reacted in either dissolution-favorable (Task 3) or precipitation-favorable conditions (Task 4) at 80° C and 77 bar for 3 weeks. The reaction conditions are summarized in **Table 3**. Synchrotron μ -XRF Fe maps (**Figure 11**) were taken at the Fe (III) edge at the energy of 7128 eV. The maps record the distribution of total Fe with a slight emphasis on Fe(III), if there's any. Figure 4 shows that total Fe distribution is similar for pre- and post-reaction Marcellus cores. EXAFS data on selective points did not show noticeable Fe(III) secondary precipitates.

Table 4: Objectives in Tasks 3&4 (a) for Quarter 4.

Goal	Status
Collect synchrotron μ -XRF Fe maps from reacted Marcellus and Eagle Ford cores	Complete
Analyze Fe and S synchrotron μ -XRF data	Complete
Collect SAXS data for cross-section shale samples	Complete
Conduct duplicate experiments	Complete
Collect and analyze XRD data from unreacted and reacted samples	in progress

Different from Marcellus cores, Eagle Ford cores reacted under dissolution-favorable conditions present a zone rich in secondary Fe species close to shale surface. This secondary Fe species was identified with EXAFS as hematite were observed near the interface. Secondary Fe(III) is produced because dissolution of carbonate increased pH of the pore water. High pH favors fast oxidation of Fe(II) to produce Fe(III), which rapidly precipitated as a secondary phase. In the Marcellus system with low carbonate content, pH remains acidic (as reported in **Quarter 3** report), and Fe(II) released from pyrite dissolution can diffuse to solution before they are oxidized. This trend of Fe(II) oxidation time scale versus carbonate content is consistent with our findings in our previous study using shale sands.

In addition to Fe redox reaction, S redox reaction is also a powerful sign of chemical reaction in shale, because pyrite dissolution release Fe(II) and S(-II), which can both be oxidized by dissolved oxygen in the fracture fluid. We can use synchrotron μ -XRF to map the micron-scale distribution of sulfate on cross-sections cut from pre- and post-reaction cores. Such measurements were performed at SSRL beamline 14-3 in March and June, and data analyses were conducted in Quarter 4 (**Figure 12**). The clay-rich New York Marcellus did not show obvious difference after reaction under both dissolution- and precipitation-favorable conditions. Surprisingly, Pennsylvania Marcellus (which is also clay-rich) showed significant oxidation of pyrite to sulfate after reacted with fracture fluid. The striking difference between New York and Pennsylvania Marcellus is attributed to the amount of microcracks in the Pennsylvania Marcellus. From the micro-CT images of both Marcellus shales shown in **Figure 10**, Pennsylvania Marcellus has microcracks, whereas New York Marcellus hardly has any microcracks. This comparison suggest that the reactivity of shale matrix is largely dependent on the abundance of microcracks in the matrix. Interestingly, however, sulfide oxidation in the Pennsylvania Marcellus was not localized to near-microcrack regions, but is distributed throughout the core, suggesting that a finer-scale pore network is present but not resolved with the micro CT in **Figure 10**.

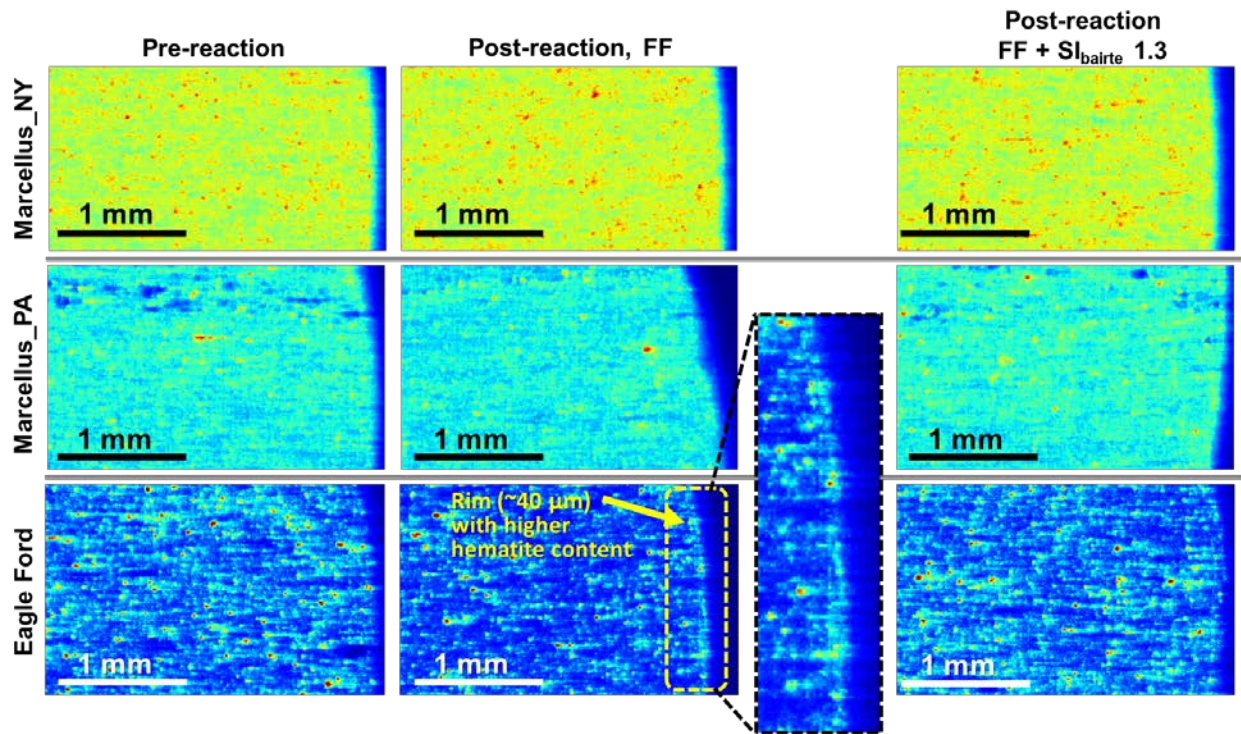


Figure 11. Synchrotron μ -XRF Fe maps on cross-sections of pre- and post-reaction cores. The Left column are pre-reaction cores, the middle column are cores reacted under dissolution-favorable condition (pH 2 fracture fluid, i.e., FF in the figure), and the right column are cores reacted under the precipitation-favorable condition (pH 2 fracture fluid with additional Ba source, $SI_{\text{barite}} 1.3$). Maps are collected at 7128 eV at the maximum intensity for Fe(III), showing total Fe(II)+Fe(III) content but with a slight emphasize on Fe(III). The warmer the color, the higher content of Fe. Marcellus shale show similar amounts of Fe on post-reaction cores compared to pre-reaction cores. Eagle Ford reacted with fracture fluid without additional Ba sources had a $\sim 40 \mu\text{m}$ rim rich in hematite close to the shale surface. This zone is not observed for the system with additional Ba source.

For Pennsylvania Marcellus reacted with fracture fluid with additional Ba^{2+} and SO_4^{2-} , a rim of sulfate-rich zone close to the shale surface ($\sim 40 \mu\text{m}$ thick) were observed, consistent with results from scoping experiments (Quarter 2 report). Interestingly, in this case S oxidation is less than that in the system without additional $\text{Ba}^{2+}/\text{SO}_4^{2-}$. We hypothesize that the reduced oxidation of sulfur in the system with additional $\text{Ba}^{2+}/\text{SO}_4^{2-}$ is due to secondary BaSO_4 precipitation on the core surface, which reduced porosity and thus reduced diffusion of O_2 from fracture fluid into the shale matrix. We will examine this hypothesis in duplicate experiments. Duplicate experiments were conducted in September using newly prepared New York and Pennsylvania Marcellus and Eagle Ford under conditions listed in **Table 3**. The post-reaction samples were collected for analyses in the Quarters 5 and 6. Experimental results that are particularly important to confirm are: (1) More barite precipitation in Eagle Ford case where carbonate dissolution buffers pH to neutral as opposed to carbonate-poor Marcellus; (2) Pyrite oxidation throughout the Pennsylvania Marcellus cores; and (3) reduced reactivity of the Pennsylvania Marcellus cores due to a thin layer of barite coating on the core surface.

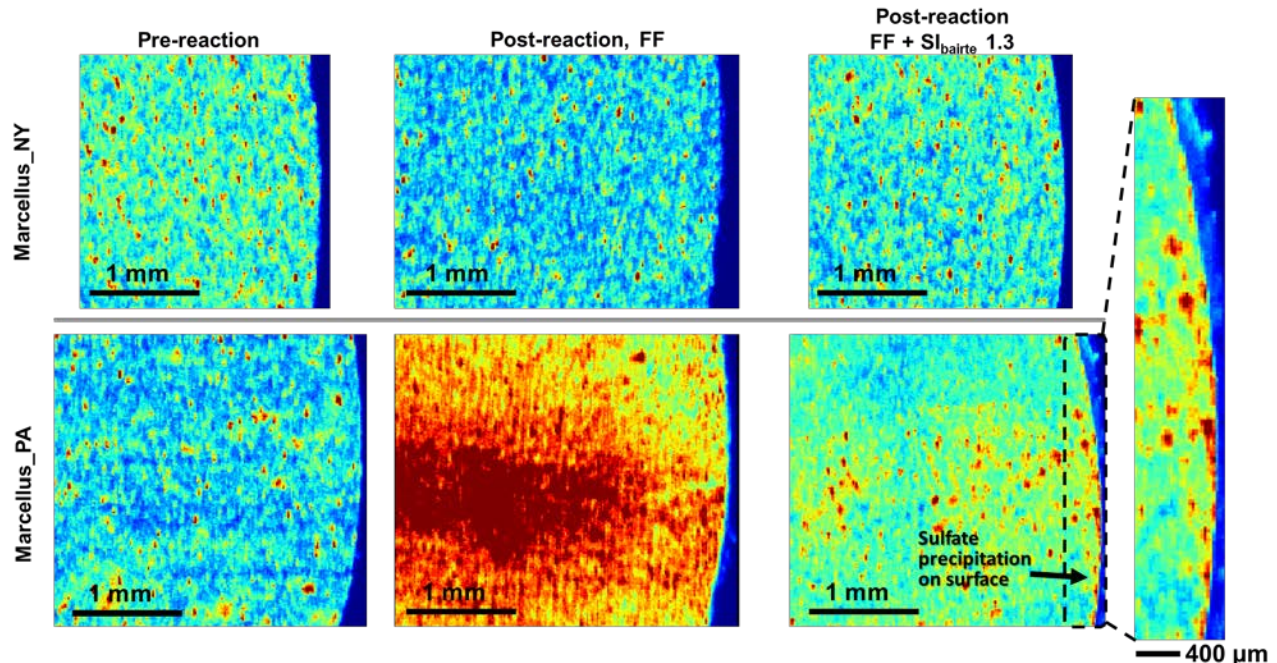


Figure 12. Synchrotron μ -XRF sulfate maps on cross-sections of pre- and post-reaction cores. Maps are collected at 2482.5 eV, *i.e.*, the energy position where inorganic sulfate has its greatest intensity. The warmer the color, the higher concentration of S species, with particular sensitivity for sulfate. If the sample is unoxidized, as is the case for the pre-reaction columns, then the maps will show the positions of pyrite. If the sample is oxidized, then the distribution of sulfur species will change and the fluorescence X-ray intensity will increase as sulfate precipitates in pore space. Based on this interpretive schema, it can be seen that New York Marcellus shale cores did not show oxidation of pyrite to sulfate. In contrast, Pennsylvania Marcellus shales show significant oxidation of sulfide to sulfate. When Ba was present in solution, then a rim of sulfate was observed to accumulate (lower-right map), indicating that BaSO_4 precipitation had occurred. Remarkably, when the barite coating was present, sulfide oxidation inside the matrix was much less extensive.

μ -XRF maps of reacted Eagle Ford cores (**Figure 13**) show BaSO_4 precipitation in the core. From the cross-section of the Eagle Ford core reacted with fracture fluid and additional $\text{Ba}^{2+}/\text{SO}_4^{2-}$, it is clear that BaSO_4 precipitation mainly occurred in microcracks, consistent with the CT data shown in Quarter 3 Report.

Planned Experiments in the next quarter.

- Analyze XRD data for pre- and post-reaction cores.
- Analyze samples from duplicate experiments.
- Measure pH and ion concentrations of post-reaction fracture fluid to understand the mechanisms of whole-core reactions.
- Collect synchrotron μ -XRF Fe data at SSRL Beamline 2-3 for duplicate experiment samples to confirm trends shown in Figure 6 .
- Collect synchrotron μ -XRF S data at SSRL Beamline 14-3 for duplicate experiment samples to confirm trends shown in Figures 7 and 8.

Manuscript plans for Tasks 3&4(a). One manuscript is planned for this task on shale matrix alterations after exposure to fracturing fluid. This manuscript will contain CT imaging data (micro- and nano-scale), XRF mapping coupled with XAS, and complementary techniques.

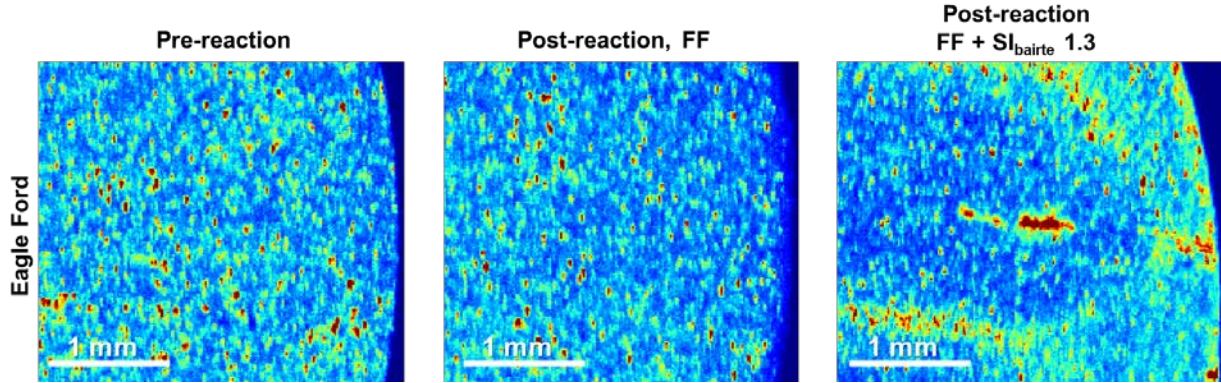


Figure 13. Synchrotron μ -XRF sulfate maps on cross-sections of pre- and post-reaction Eagle Ford cores. Maps are collected at 2482.5 eV, *i.e.*, at the maximum intensity of the inorganic sulfate peak. The warmer the color, the higher concentration for S species.

6. Task 3&4 (b): Measuring permeability alteration induced by fracture fluid reaction

From the point view of gas production, alteration of fracture surface microstructure alters matrix permeability and thus production. In this section we are conducting permeability measurements before and after dissolution-favorable and precipitation-favorable experiments, followed by microscale characterization. Currently, we are aiming to measure permeability on 2 shale gas samples from the Eagle Ford formation and the Marcellus formation.

Table 4: Objectives in Tasks 3&4 (a) for Quarter 3 & 4.

Goal	Status
Collect permeability measurements for unreacted Eagle Ford and Marcellus microcores	Complete
React Eagle Ford microcore in fracture fluid	Complete
Collect permeability measurement for reacted Eagle Ford microcore	in progress

Progress in Quarters 3 and 4

New Marcellus-PA and Eagle Ford shale microcores (10mm diameter) were cored from 1-inch cores. Permeability measurements using the gas pulse-decay method were completed on both unreacted shale microcore. We performed a total of 4 pulse decay measurements on the Eagle Ford microcore, where 3 pulse tests were set at pore pressures 200psi, 400psi, 800psi, while maintaining a constant effective pressure of 500psi across all pulse tests, in order to calculate the intrinsic permeability (K_{∞}) and effective pore width of the microcore using the

Klinkenberg analysis [14]. The final pulse was set to pressure conditions (pore pressure = 2000psi, with an effective pressure = 1000psi) to gauge relative well production conditions. Our results show the Eagle Ford microcore measured permeability to be in the nanodarcy range (45nd, 34nd, 23nd) for increasing pore pressures 200psi, 400psi, 800psi. In which, the intrinsic permeability was estimated to be 18nd, while the effective pore width was estimated to be 12nm (**Figure 14**).

We attempted to repeat the same pressure sequence for permeability measurements on the Marcellus microcore, but found that the measured permeability of the first pulse test (pore pressure=200psi) was impermeable after saturating the microcore for 8 days continuous and performing pulse decay test for 6 days with no measurable change in the pressure front along the microcore (**Figure 15**).

Lessons learned. After completing the baseline permeability measurements on the unreacted microcores, it became clear that the presence of microfractures is important for measuring permeability. The Eagle Ford microcore had many microfractures present which helped with permeability measurements. In contrast, the Marcellus microcore was relatively devoid of microfractures and was essentially impermeable over the span of the experiment. Moreover, because of the ultra-low permeability in these shale gas samples, pulse experiments are taking a longer time than originally planned and at times over 8 days, while maintaining a leak-free system in order to detect the small pressure change across the measured microcore sample. Our observations here are consistent with the findings reported in Task 3&4(a), *i.e.*, that microfractures are important for chemical diffusivity transport and are needed in order for the development of an altered zone from the fracture fluid reaction.

Our original experimental strategy was to use shale microcores to allow CT characterization and synchrotron measurements on the exact same cores as the permeability measurements. However, we have found that small cores tend to have fewer microfractures. The smaller the core, the fewer the microfractures present.

Our experience in the last 2 quarters has taught us that it is impractical to combine permeability measurements on microcores with direct CT characterization. In order to keep the experimental program on-schedule, we are taking the following steps to speed up and streamline permeability measurement: (a) Strategically identify a minimal set of cores required to establish scientific results; (b) Implement a single workflow that minimizes procedural steps during the pulse decay measurement and that enables longer times for cores to respond to pressure pulses during each step; (c) Use 1 inch-diameter cores because they have higher permeability than micro-cores (and hence faster measurement time); (d) React cores with fracture fluid 'off line' and bring them to the core-flood apparatus only to measure permeability (*i.e.*, do not use the permeameter apparatus to react cores with fracture fluid).

Planned Experiments in the next quarter. After completing the permeability measurements on the unreacted cores, we will perform the frac fluid reactions on the unreacted cores and plan to measure the permeability of the reacted cores to assess the impact of secondary porosity enhancement or decline on the shale rock matrix.

We will also repeat the permeability measurements on the unreacted 1-inch cores to compare the relative change in permeability of both samples along different sample sizes. This will give us

an indication on the change in effective pore width of the shale rock matrix as a function of sample size and microfracture/texture distribution.

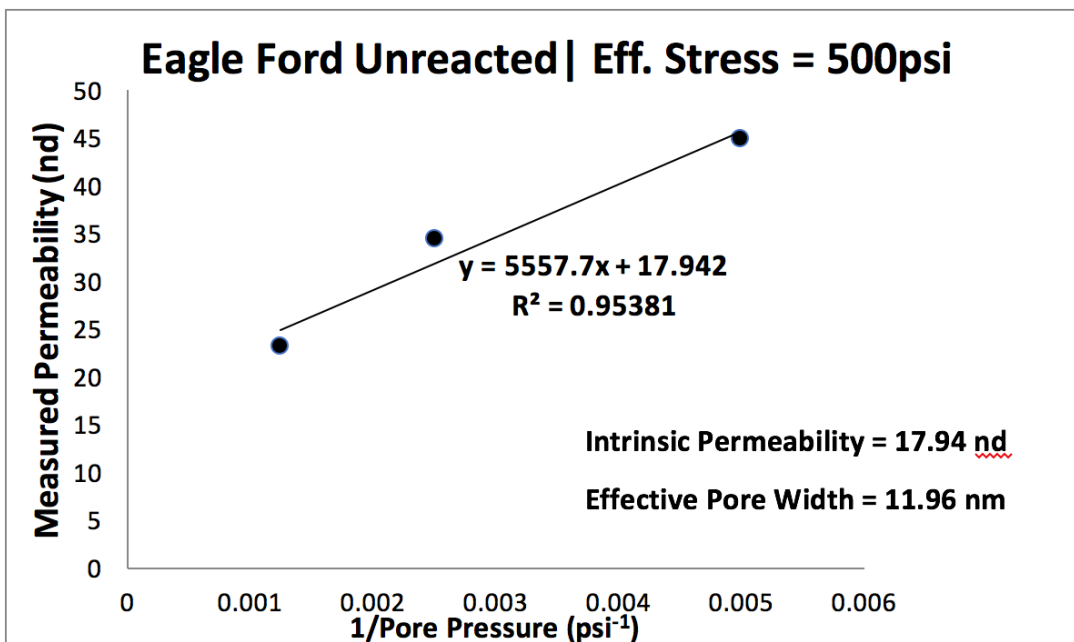
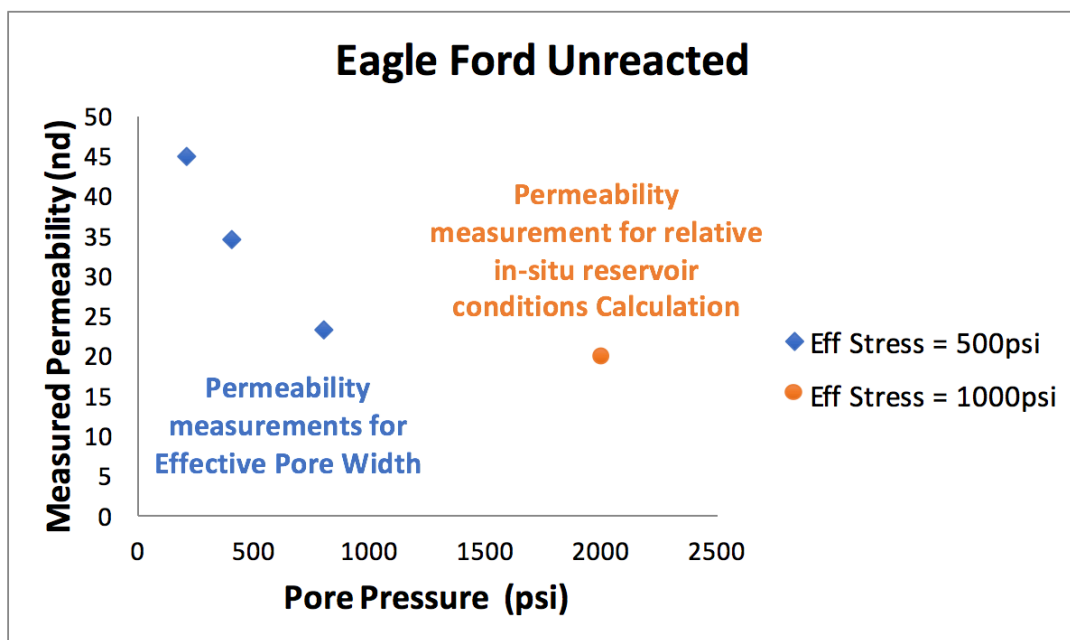


Figure 14. Top: Measured Permeability for Eagle Ford microcore along increasing pore pressure steps while maintaining constant effective pressure. Bottom: Klinkenberg Analysis to calculate both intrinsic permeability (K_{∞}) and effective pore width.

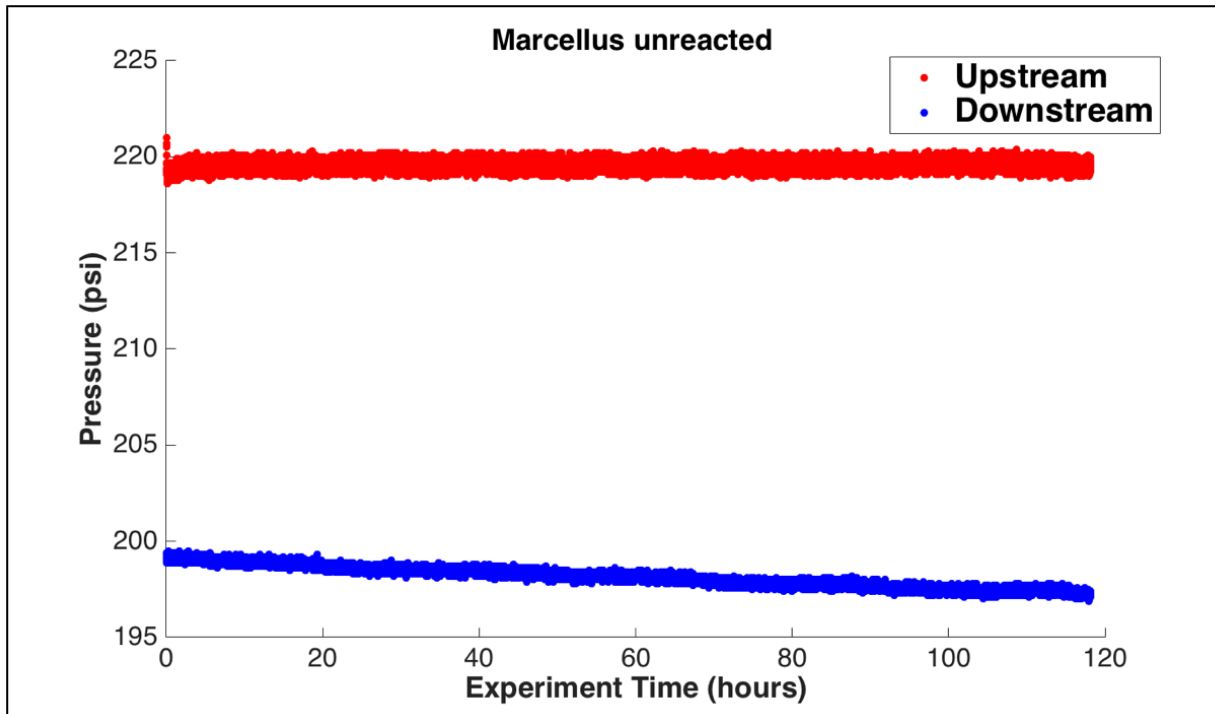


Figure 15. Pressure reading for both upstream and downstream sides of pore pressure system during permeability measurement at pore pressure = 200psi of Marcellus microcore. The pressure along the downstream has not increased over the span of 6 days since the beginning of the pulse test. Since we weren't able to measure permeability, we are not able to compute both the intrinsic impermeability and the effective pore width.

Manuscript Plans for Tasks 3&4(b). One manuscript is planned for these tasks detailing the alterations permeability of shale cores when reacted to hydraulic fracturing solution. This manuscript will contain CT imaging data and pulse decay permeability measurement.

7. References:

- [1] Krauss, C. *Boom in American Liquefied Natural Gas Is Shaking Up the Energy World*. New York Times Article, published Oct 16, 2017.
- [2] Ghode, Roopali; Muley, Rajashree; Sarin, Rajkamal. *Operationally determined chemical speciation of barium and chromium in drilling fluid wastes by sequential extraction*. *Chemical Speciation & Bioavailability*, 7 (4) **1995**, 133-137.
- [3] Neff, Jerry M. *US EPA Report: Fate and biological effects of oil well drilling fluids in the marine environment: A literature review*. **1981**, 1-178.
- [4] Neff, Jerry M. *Estimation of bioavailability of metals from drilling mud barite*. *Integrated Environmental Assessment and Management*. 4 (2) **2008**, 184-193.
- Kerr, R.A. *Natural Gas from shale bursts onto the scene*. *Science*, 328, **2010**, 1624-1626.
- [5] Renock, Devon; Landis, Joshua D.; Sharma, Mukul. *Reductive weathering of black shale and release of barium during hydraulic fracturing*. *Applied Geochemistry*, 65, **2016**, 73-86.
- [6] Jew, A. D.; Dustin, M. K.; Harrison, A. L.; Joe-Wong, C.; Thomas, D. L.; Maher, K.; Gordon E. Brown, J.; Bargar, J. R., *Importance of pH, Oxygen, and Bitumen on the Oxidation and Precipitation of Iron during Hydraulic Fracturing of Oil/Gas Shales*. *Energy & Fuels* DOI: 10.1021/acs.energyfuels.6b03220
- [7] Akob, D.M.; Cozzarelli, I.M.; Dunlap, D.S.; Rowan, E.L.; Lorah, M.M. *Organic and Inorganic Composition and Microbiology of Produced Waters from Pennsylvania Shale Gas Wells*. *Applied Geochemistry*, 60, **2015**, 116-125
- [8] Lester, Y.; Ferrer, I.; Thurman, E.M.; Sitterley, K.; Korak, J.A.; Aiken G.; Linden, K.G. *Characterization of Hydraulic Fracturing Flowback Water in Colorado: Implications for Water Treatment*. *The Science of the Total Environment*, 512-513, **2015**, 637-644.
- [9] Dai, Chong; Stack, Andrew G.; Koishi, Ayumi; Fernandez-Martinez, Alejandro; Lee, Sang Soo; Hu, Yandi. *Heterogeneous Nucleation and Growth of Barium Sulfate at Organic-Water Interfaces: Interplay between Surface Hydrophobicity and Ba²⁺ Adsorption*. *Langmuir*, 32, **2016**, 5277-5284.
- [10] Kugler, Ricco T.; Beibert, Katharina; Kind, Matthias. *On heterogeneous nucleation during the precipitation of barium sulfate*. *Chemical Engineering Research and Design*, 114, **2016**, 30-38.
- [11] Zhen-Wu, B.Y.; Dideriksen, K.; Olsson, J.; Raahauge, P.J.; Stipp, S.L.S.; Oelkers, E.H. *Experimental determination of barite dissolution and precipitation rates as a function of temperature and aqueous fluid composition*. *Geochimica et Cosmochimica Acta*, 194, **2016**, 193-210.
- [12] Jones, F.; Piana, S.; Gale, J.D. *Understanding the kinetics of barium sulfate precipitation from water and water-methanol solutions*. *Crystal Growth & Design*, 8 (3), **2008**, 817-822.
- [13] Smith, E.; Hamilton-Taylor, J.; Davison, W.; Fullwood, N.J.; McGrath, M. *The effect of humic substances on barite precipitation-dissolution behaviour in natural and synthetic lake waters*. *Chemical Geology*, 27, **2004**, 81-89.
- [14] Heller, R.; Vermilyen, J.; Zoback, M. *Experimental investigation of matrix permeability of gas shales*. *AAPG Bulletin*, 98 (5) **2014**, 975-995.

8. RISK ANALYSIS

Task 1: No significant risks to report

Task 2: No significant risks to report

Task 3&4. Understand fundamental precipitation and dissolution reactions in shale cores and determine shale matrix permeability changes by these reactions

Technical risks:

Risk 1. Natural rock samples may produce different results due to heterogeneity in the rock matrix.

Risk 2. Preliminary SAXS data analyses suggest that scattering signals from nanopores may be lower than the scattering from larger pores.

Risk 3. Shale matrix has very low permeability and takes long time to give response to a pressure pulse on the up-stream, thus may significantly increase our measurement time.

Mitigation:

- (i) *Risk 1. Duplicate experiments produce different results due to heterogeneity in natural rocks*

Mitigation: Run additional experiments with shale samples from the same bulk core. To maximize the number of duplicates we can run using the same bulk core (where small cores are drilled from), these duplicate samples may be irregular in geometry.

- (ii) *Risk 2. SAXS intensities from small pores may be hard to be separated from the large pores and fractures, rendering it hard to compare pore structure at multiscale.*

Mitigation 1: Grind the reacted region from the reacted shale cores to powder to minimize micrometer pores, facilitating analyses on the nanometer pores.

Mitigation 2: Collect CT data from SSRL synchrotron x-ray beamline 2-2 at $< 2 \mu\text{m}$ pixel size, and compare with the CT data collected from Zeiss Xradia 520 Versa X-ray CT with μm pixel size to obtain the difference in pore structure at multiscale.

- (iii) *Risk 3. Permeability tests take a long time.*

Mitigation: Several steps are being implemented: (a) Strategically identify a minimal set of cores required to establish scientific result; (b) Implement a single workflow that minimizes procedural steps during the pulse decay measurement, which enables longer times for cores to respond to pressure pulses during each step; (c) Use 1 inch-diameter cores because they have higher permeability than micro-cores (and hence faster measurement time); (d) React cores with fracture fluid 'off line' and bring them to the core-flood apparatus only to measure permeability (*i.e.*, do not use the permeameter apparatus to react cores with fracture fluid); and (e) Purchase additional pumps and core holders to expand experimental facility availability (this option has not yet been implemented).

9. MILESTONE STATUS

Activity and milestones	Verification method [†]	Planned Milestone Date	Actual completion or status
Task 1. Project management			
1.1 Development of PMP	D	10-31-16	10-28-16
1.2 Recruit postdoc / RA	D	4-30-17	10-30-17
1.3 Quarterly research performance reports	D	1-30-17‡	7-30-17
1.4 Annual research performance report	D	11-30-17*	11-30-17
1.5 Final technical report	D	11-30-18	
Task 2. Influence of dissolved organic compounds on precipitate formation/stability			
2.1 Research/evaluation of literature and detailed experimental design	D	1-30-17	12-23-16
2.2 Set-up and test stirred tank reactors	D	1-30-17	12-19-16
2.3 Complete initial scoping experiments to determine types of organic compounds for detailed measurement	D	4-30-17	3-13-17
2.4 Complete measurements of initial rates of solid precipitation	D	7-30-17	6-30-17
2.5 Identification of precipitate mineralogy	XRD, XAS, SEM	10-30-17	9-30-17
2.6 Complete measurement of shale sand dissolution	D	7-30-17	6-30-17
2.7 Complete solubility measurements	D	7-30-17	10-30-17
2.8 Dissolution rate measurements in presence of shale sands with coupled dissolution and precipitation	D	10-30-17	10-30-17
2.9 Complete initial draft of manuscript	D	4-30-18	In progress
2.10 Submit manuscript	D	7-30-18	
Task 3. Impact of secondary pore networks on gas transport across shale matrix-fracture interfaces			
3.1 Research/evaluation of literature and design experiments favorable for secondary porosity generation	D	1-30-17	12-21-16
3.2 Submit beam time proposals	D	1-30-17	12-1-16
3.3 Acquire shale samples	D	1-30-17	11-9-16
3.4 Conduct telecons quarterly (as needed) with NETL group	N	1-30-17‡	Ongoing
3.5 Conduct telecons quarterly (as needed) with LANL group	N	1-30-17‡	Ongoing
3.6 Mineralogical characterization of shale samples	XRD, SEM	7-30-17	6-30-17
3.7 Measure gas permeability of unreacted cores	P	7-30-17	7-30-17
3.8 Collect μ -CT images for unreacted shale cores	μ -CT	7-30-17	3-7-17
3.9 Complete image processing for unreacted shale cores	D	10-30-17	10-30-17
3.10 Set up and test whole-core reactors: initial scoping experiments	D	7-30-17	11-30-16
3.11 Perform shale whole-core reactions	D	1-30-18	12-19-16
3.12 Collect μ -CT images on reacted cores	μ -CT	4-30-18	in progress
3.13 Collect XRM maps on thin section of unreacted and reaction cores	XRM, SEM	4-30-18	in progress
3.14 Measure gas permeability through reacted cores	P	4-30-18	in progress
3.15 Complete image processing and data analysis for reacted cores	D	7-30-18	
3.16 Develop numerical model to describe dependency of gas transport across shale-fracture interface on secondary pore network	D	7-30-18	in progress
3.17 Complete initial draft of manuscript	D	7-30-18	
3.18 Submit manuscript	D	10-30-18	
Task 4. Impact of secondary precipitation on gas transport across shale matrix-fracture interfaces			

Activity and milestones	Verification method[†]	Planned Milestone Date	Actual completion or status
4.1 Research/evaluation of literature and design experiments favorable for secondary precipitation	D	1-30-17	12-21-16
4.2 Measure gas permeability of unreacted cores	P	7-30-17	in progress
4.3 Collect μ -CT images on unreacted shale cores	μ -CT	7-30-17	3-7-17
4.4 Complete image processing and analysis on unreacted shale cores	D	10-30-17	in progress
4.5 Set up and test whole-core reactors: initial scoping experiments	D	10-30-17	3-20-17
4.6 Perform shale whole-core reactions	D	4-30-18	in progress
4.7 Measure permeability of reacted cores	D	7-30-18	in progress
4.8 Collect μ -CT images on reacted cores	P, μ -CT	10-30-18	in progress
4.9 Collect XRM maps on thin section of unreacted and reaction cores	XRM, SEM	10-30-18	in progress
4.10 Complete image processing and data analysis for reacted cores	D	1-30-19	
4.11 Develop numerical model to describe dependency of gas transport across shale-fracture interface on secondary precipitation	NM	10-30-18	

[‡] Quarterly reports will follow every 3 months following starting date. * Annual reports are due every 12 months on Nov 30.

[†] Verification Method Key:

AF	=	Software for data processing and visualization (Avizo Fire)
D	=	Documentation or data
EELS	=	Electron energy loss spectroscopy
FIB-SEM	=	Focused ion beam – scanning electron microscopy
μ -CT	=	Micrometer-scale X-ray computed tomography
nano-CT	=	Nanometer-scale X-ray computed tomography
N	=	Note from meeting
NM	=	Numerical modeling
OP	=	Optical petrography
P	=	Pulse-decay permeability
SAXS	=	Small angle X-ray scattering
SANS	=	Small angle neutron scattering
SEM	=	Scanning electron microscopy
TEM	=	Transmission electron microscopy
TXMWiz	=	Software for data processing of transmission X-ray images (TXM Wizard)
XAS	=	X-ray absorption spectroscopy
XRM	=	X-ray microprobe
XRD	=	X-ray diffraction

10. SCHEDULE STATUS

All milestones for this quarter have been met and there are no changes to the experimental program. The project is on-schedule.

Modification explanation log for milestones list:

Date	Task	Modification	Explanation
11-30-17		No modifications	

11. COST STATUS

Baseline Reporting Quarter		Cost Plan/Status																			
		Year 1	Year 2		Year 3		Year 4		Year 5		Start: 10/1/17	End: 9/30/18									
Q1	Q2	Q3	Q4	Q5	Q6	Q7	Q8	Q9	Q10	Q11	Q12	Q13	Q14	Q15	Q16	Q17	Q18	Q19	Q20		
Baseline Cost Plan																					
Task 1				\$ 2,709	\$ 3,195	\$ 4,744	\$ 14,453	\$ 8,846	\$ 8,846	\$ 8,846	\$ 8,846	\$ 9,686	\$ 9,686	\$ 9,686	\$ 9,686	\$ 12,750	\$ 12,750	\$ 12,750	\$ 12,750	\$ 12,750	
Task 2				\$ 5,743	\$ 6,773	\$ 10,058	\$ 30,641	\$ 14,941	\$ 12,105	\$ 12,105	\$ 12,105	\$ 31,681	\$ 31,681	\$ 31,681	\$ 31,681	\$ 44,625	\$ 44,625	\$ 44,625	\$ 44,625	\$ 44,625	\$ 44,625
Task 3				\$ 4,931	\$ 5,815	\$ 8,635	\$ 26,305	\$ 10,292	\$ 10,292	\$ 10,292	\$ 10,292	\$ 42,400	\$ 42,400	\$ 42,400	\$ 42,400	\$ 35,700	\$ 35,700	\$ 35,700	\$ 35,700	\$ 35,700	\$ 35,700
Task 4				\$ 5,743	\$ 6,773	\$ 10,058	\$ 30,641	\$ 12,165	\$ 12,165	\$ 12,165	\$ 12,165	\$ 23,733	\$ 23,733	\$ 23,733	\$ 23,733	\$ 34,425	\$ 34,425	\$ 34,425	\$ 34,425	\$ 34,425	\$ 34,425
Task 5				\$ 5,743	\$ 6,773	\$ 10,058	\$ 30,641	\$ 12,165	\$ 12,165	\$ 12,165	\$ 12,165										
Task 6				\$ 2,221	\$ 2,620	\$ 3,890	\$ 11,852	\$ 5,964	\$ 5,964	\$ 5,964	\$ 5,964										
Non-Federal Share																					
Total Planned Costs (Federal and Non-Federal)																					
Cumulative Baseline Cost	\$ -	\$ -	\$ -	\$ -	\$ 27,091	\$ 59,040	\$ 106,484	\$ 251,017	\$ 315,390	\$ 376,927	\$ 438,464	\$ 540,000	\$ 647,500	\$ 755,000	\$ 862,500	\$ 970,000	\$ 1,097,500	\$ 1,225,000	\$ 1,352,500	\$ 1,480,000	
Actual Incurred Costs																					
Task 1				\$ 2,709	\$ 3,195	\$ 4,744	\$ 14,453	\$ 8,846	\$ 8,846	\$ 8,846	\$ 8,846	\$ 9,686	\$ 9,686	\$ 9,686	\$ 9,686	\$ 12,750	\$ 12,750	\$ 12,750	\$ 12,750	\$ 12,750	
Task 2				\$ 5,743	\$ 6,773	\$ 10,058	\$ 30,641	\$ 12,323	\$ 10,852	\$ 11,143	\$ 14,671	\$ 25,514	\$ 47,023	\$ 29,782	\$ 57,855	\$ (7,869)					
Task 3				\$ 4,931	\$ 5,815	\$ 8,635	\$ 26,305	\$ 10,579	\$ 9,316	\$ 9,566	\$ 12,995	\$ 20,411	\$ 37,622	\$ 23,626	\$ 46,284	\$ (5,815)					
Task 4				\$ 5,743	\$ 6,773	\$ 10,058	\$ 30,641	\$ 12,323	\$ 10,852	\$ 11,143	\$ 14,671	\$ 19,682	\$ 36,279	\$ 22,975	\$ 44,631	\$ (5,607)					
Task 5				\$ 5,743	\$ 6,773	\$ 10,058	\$ 30,641	\$ 12,323	\$ 10,852	\$ 11,143	\$ 14,671	\$ -	\$ -	\$ -	\$ -	\$ -	\$ -	\$ -	\$ -	\$ -	
Task 6				\$ 2,221	\$ 2,620	\$ 3,890	\$ 11,852	\$ 4,766	\$ 4,197	\$ 4,310	\$ 5,675	\$ -	\$ -	\$ -	\$ -	\$ -	\$ -	\$ -	\$ -	\$ -	
Non-Federal Share																					
Total Incurred Costs - Quarterly (Federal and Non-Federal)																					
Cumulative Incurred Cost	\$ -	\$ -	\$ -	\$ -	\$ 27,091	\$ 31,949	\$ 47,444	\$ 144,533	\$ 58,127	\$ 51,187	\$ 52,562	\$ 69,204	\$ 72,898	\$ 134,366	\$ 85,093	\$ 165,300	\$ (20,768)	\$ -	\$ -	\$ -	
Variance																					
Task 1				\$ -	\$ -	\$ -	\$ -	\$ -	\$ 3,033	\$ 3,727	\$ 3,589	\$ 1,925	\$ 2,396	\$ (3,750)	\$ 1,177	\$ (6,843)	\$ 14,827	\$ 12,750	\$ 12,750	\$ 12,750	
Task 2				\$ -	\$ -	\$ -	\$ -	\$ -	\$ 2,618	\$ 1,253	\$ 962	\$ (2,566)	\$ 6,167	\$ (15,347)	\$ 1,899	\$ (26,174)	\$ 51,894	\$ 44,625	\$ 44,625	\$ 44,625	
Task 3				\$ -	\$ -	\$ -	\$ -	\$ -	\$ (287)	\$ 976	\$ 725	\$ (2,303)	\$ 21,988	\$ 4,777	\$ 18,574	\$ (3,884)	\$ 41,515	\$ 35,700	\$ 35,700	\$ 35,700	
Task 4				\$ -	\$ -	\$ -	\$ -	\$ -	\$ (188)	\$ 1,313	\$ 1,022	\$ (2,506)	\$ 4,690	\$ (12,546)	\$ 798	\$ (20,888)	\$ 40,932	\$ 34,425	\$ 34,425	\$ 34,425	
Task 5				\$ -	\$ -	\$ -	\$ -	\$ -	\$ (158)	\$ 1,313	\$ 1,022	\$ (2,506)	\$ -	\$ -	\$ -	\$ -	\$ -	\$ -	\$ -	\$ -	
Task 6				\$ -	\$ -	\$ -	\$ -	\$ -	\$ -	\$ -	\$ -	\$ -	\$ -	\$ -	\$ -	\$ -	\$ -	\$ -	\$ -	\$ -	
Non-Federal Share				\$ -	\$ -	\$ -	\$ -	\$ -	\$ -	\$ -	\$ -	\$ -	\$ -	\$ -	\$ -	\$ -	\$ -	\$ -	\$ -	\$ -	\$ -
Total Variance - Quarterly (Federal and Non-Federal)	\$ -	\$ -	\$ -	\$ -	\$ -	\$ -	\$ -	\$ -	\$ 6,245	\$ 16,595	\$ 25,569	\$ 17,902	\$ 52,503	\$ 25,638	\$ 48,046	\$ (9,755)	\$ 138,513	\$ 266,013	\$ 399,513	\$ 521,013	
Cumulative Variance	\$ -	\$ -	\$ -	\$ -	\$ -	\$ -	\$ -	\$ -	\$ 6,245	\$ 16,595	\$ 25,569	\$ 17,902	\$ 52,503	\$ 25,638	\$ 48,046	\$ (9,755)	\$ 138,513	\$ 266,013	\$ 399,513	\$ 521,013	

12. Collaborative Leveraging: The project effort is supported by 2 collaborating postdoctoral fellows (Arjun Kholi and Andy Kiss, both SLAC), funded by a non-NETL program. We are currently collaborating with 1 Ph.D. student in the Zoback research group as well as 1 Ph.D. student in the Kavscek research group at Stanford University. Additional, collaboration is ongoing with the Hakala and Lopano groups at NETL.

13. CONCLUSIONS

We made significant process toward our two main goals in the past year. Goal 1 was to discover, quantify, and develop models for fundamental geochemical controls over barite scale precipitation. Ionic strength (I.S.) does have a strong impact on barite solubility. However, pH was found to be the dominant parameter controlling barite precipitation. In all systems containing organics, barite precipitation was never halted. This finding demands a rethinking of the use of organic scale inhibitors in hydraulic fracturing systems. Due to the significant problems producers have with barite scale precipitation and its potential of substantially reducing production from wells, new research into optimizing fracture fluid recipes for various shale plays needs to be done.

Moreover, we found that drilling mud is likely to be an important in not the most important source of Ba released into fracture fluid. Indeed, significantly more Ba from drilling mud over a 72 hr reaction time than was released from either pure barite or any of the shale samples over a 3-week reaction time. We attribute the greater release of Ba was released from drilling mud to the presence of organics, coupled with low pH conditions present. This finding suggests that reducing Ba²⁺ release from drilling mud may be a more effective scale inhibition strategy than trying to prevent barite precipitation after Ba has already been released to injected fluids in shale.

Goal 2 was to discover, quantify, and develop models for the altered zone at shale-fluid interfaces, through which gas and oil must pass in order to be produced from wells. Our work shows that the altered zone is much thicker than previously thought, with thickness exceeding 0.5 cm. The thickness and reactivity of the altered layer was strongly controlled by two key factors: the abundance of microfractures in the shale core, and (ii) the presence of scale precipitation. A layer of scale ≤ 50 microns thick dramatically attenuated diffusive exchange of solutes between fracture solution and the shale matrix. These findings emphasize the highly deleterious impact of scale precipitation on porosity and pore connectivity.

Overall, our results suggest a new conceptual model for understanding scale formation in unconventional shales. Acidification of shales will cause scale-forming solutes to be released from drilling muds (Ba, Ca) and shales (Fe, Ca, Al) early in the stimulation process. Subsequent neutralization of this acid as shale minerals dissolve will create conditions favorable to scale precipitation and loss of permeability. The extent of scale precipitation will vary in response to geochemical conditions present, such as carbonate concentration. This conceptual model provides a clear basis for modifying stimulation procedures to minimize formation damage and improve long-term primary recovery.

APPENDIX A. Deliverables

Publications during the performance period

1. Harrison, A.L., Jew, A.D., Dustin, M.K., Thomas, D.L., Joe-Wong, C.M., Bargar, J.R., Johnson, N., Brown, G.E., Jr., and Maher, K. (2017) Element release and reaction-induced porosity alteration during shale-hydraulic fracturing fluid interactions. *Applied Geochemistry* 82: p.47-62. <https://doi.org/10.1016/j.apgeochem.2017.05.001>.
2. Jew, A.D., Harrison, A.L., Dustin, M.K., Joe-Wong, C., Thomas, D.L., Maher, K., Brown, G.E., D. Cercone, and Bargar, J.R. (2017) Mineralogical and Porosity Alteration Following Fracture Fluid-Shale Reaction. *Unconventional Resources Technology Conference Proceedings*. DOI 10.15530/urtec-2017-2708858.
3. Jew, A.D., Harrison, A.L., Dustin, M.K., Harrison, A.L., Joe-Wong, C.M., Thomas, D.L., Brown, G.E., Jr., Maher, K., and Bargar, J.R. (2017) Impact of organics and carbonates on the oxidation and precipitation of iron during hydraulic fracturing of shale. *Energy and Fuels* 31: 3643–3658. 10.1021/acs.energyfuels.6b03220.

*Presentations at scientific meetings ([†]invited, *presenting author)*

1. Li, Q., Jew, A.D. Kohli, A.H., Alalli, G., Kiss, A.M. Kovscek, A.R., Zoback, M.D. Brown, G.E., Jr., Maher, K., Bargar, J.R. Pyrite Oxidation in Shale Matrices after Exposure to Fracture Fluid. Presented the 2017 SSRL User's Meeting, SLAC National Accelerator Laboratory, Menlo Park, California, Sept. 27-29, 2017 [poster]
2. Bargar, J.R., Jew, A.D., Harrison, A.L., Kohli, A., Kiss, A., Li, Q.L., Maher, K., and Brown, G.E., Jr. Geochemistry of Shale-Fluid Reactions at Pore and Fracture Scales. Presented the 2017 Goldschmidt Geochemistry conference, Paris, France, Aug, 16, 2017 [invited]
3. Li, Q., Jew, A., Harrison, A. Kohli, A.L Kiss, A. and Brown, G.E., Jr. (2017) Alteration of Porosity and Permeability within a Shale Matrix during Hydraulic Fracturing. Presented the 2017 Goldschmidt Geochemistry conference, Paris, France, Aug, 15, 2017 [poster]
4. Bargar, J.R., Jew, A.D., Harrison, A.L., Kiss, A., Kohli, A., Li, Q., Maher, K., and Brown, G.E. Jr. Pore Scale Control of Gas and Fluid Transport at Shale Matrix-Fracture Interfaces. Presented at the 2017 Mastering the Subsurface Through Technology, Innovation and Collaboration: Carbon Storage and Oil and Natural Gas Technologies Review Meeting, Pittsburgh, PA, Aug 1, 2017 [oral]
5. Bargar, J.R., Jew, A.D., Harrison, A.L., Kiss, A., Kohli, A., Li, Q., Maher, K., and Brown, G.E. Jr. (2017) Geochemistry of Shale-Fluid Reactions at Pore and Fracture Scales. Presented at the 2017 Mastering the Subsurface Through Technology, Innovation and Collaboration: Carbon Storage and Oil and Natural Gas Technologies Review Meeting, Pittsburgh, PA, Aug 2, 2017 [poster]
6. Jew, A.D., Harrison, A.L., Dustin, M.K., Joe-Wong, C., Thomas, D.L., Maher, K., Brown, G.E., D. Cercone, and Bargar, J.R. (2017) Mineralogical and Porosity Alteration Following Fracture Fluid-Shale Reaction. *Unconventional Resources Technology Conference Proceedings*. DOI 10.15530/urtec-2017-2708858. [oral]

7. Bargar, J.R., Jew, A.D., Harrison, A.L., Kiss, A., Kohli, A., Li, Q., Maher, K., and Brown, G.E. Jr. Gas and Fluid Transport at Shale Matrix-Fracture Interfaces, Presented at the National Energy Technology Laboratory, Morgantown, PA, Mar 21, 2017 [oral]
8. Kiss, A.M., Kohli, A.H., Harrison, A.L., Jew, A.D., Lim, J.H., Liu, Y., Maher, K.M., Zoback, M.D., Brown, G.E., Jr. and Bargar, J.R. (2016) 4D synchrotron X-ray imaging to understand porosity development in shales during exposure to hydraulic fracturing fluid. Presented at the American Geophysical Union Fall Meeting, Symposium H11E, Fluid-Rock Interactions Controlling Structure, Flow, and Transport in the Subsurface I, San Francisco, USA, December 12-16. [oral]
9. Harrison, A.L., Maher, K., Jew, A.D., Dustin, M.K., Kiss, A.M., Kohli, A.H., Thomas, D.L., Joe-Wong, C., Brown G.E., Jr., and Bargar, J.R. (2016) The Impact of Mineralogy on the Geochemical Alteration of Shales During Hydraulic Fracturing Operations. Presented at the American Geophysical Union Fall Meeting, Symposium H21J, Fluid-Rock Interactions Controlling Structure, Flow, and Transport in the Subsurface IV, San Francisco, USA, December 12-16. [oral]
10. Jew, A.D., Dustin, M.K., Harrison, A.L., Joe-Wong, C., Thomas, D.L., Maher, K., Brown Jr., G.E., and Bargar, J.R. (2016) The Importance of pH, Oxygen, and Bitumen on the Oxidation and Precipitation of Fe(III)-(oxy)hydroxides during Hydraulic Fracturing of Oil/Gas Shales. Presented at the American Geophysical Union Fall Meeting, Symposium H21J, Fluid-Rock Interactions Controlling Structure, Flow, and Transport in the Subsurface IV, San Francisco, USA, December 12-16. [oral]